EXAMENSARBETE I GEOLOGI VID LUNDS UNIVERSITET

Mineralogi och petrologi

Sveconorwegian influence on the ca. 1.36 Ga old Tjärnesjö granite, and associated pyroxene bearing quartz-monzonites in southwestern Sweden

Jenny Andersson

Lund 1996 Examensarbete, 20 p Nr 67
Geologiska Institutionen, Lunds Universitet

CODEN: SE-LUNBDS/NBGO-96/5067+26s

EXAMENSARBETE I GEOLOGI VID LUNDS UNIVERSITET

Mineralogi och petrologi

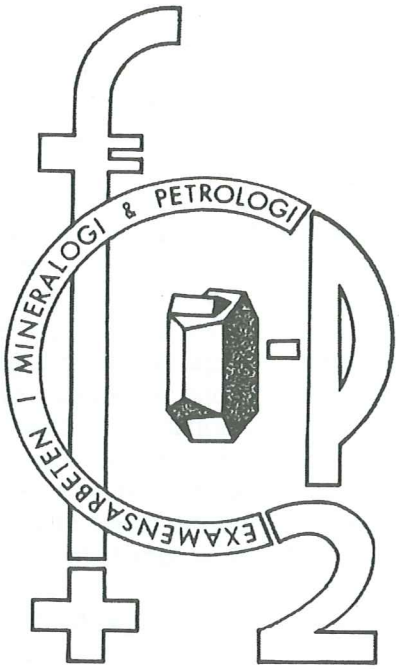

Sveconorwegian influence on the ca. 1.36 Ga old Tjärnesjö granite, and associated pyroxene bearing quartz-monzonites in southwestern Sweden

Jenny Andersson

Lund 1996 Examensarbete, 20 p Nr 67
Geologiska Institutionen, Lunds Universitet

Sveconorwegian influence on the ca. 1.36 Ga old Tjärnesjö granite, and associated pyroxene bearing quartz-monzonites in southwestern Sweden.

Abstract

The granite massif in the Tjärnesjö area, southwestern Sweden, was deformed and metamorphosed under granulite facies conditions in late Sveconorwegian time. The intrusive is dominated by a coarse-grained, megacrystic orthoclase granite. Pb-Pb evaporation datings on single zircons from the granite yield an age of ca. 1.36 Ga, interpreted as the intrusion age. A similar age was obtained on zircons from quartz-monzonitic pyroxene bearing parts within the granite, here referred to as charnockitoids. Correlations with the ca. 1.38 Ga Torpa granite and its charnockitic associations in the Varberg region further to the west are supported by the intrusion-age of the Tjärnesjö granitoids, as well as the textural and chemical character of the two intrusives.

Rocks within the Tjärnesjö massif vary from almost massive, to intensely deformed, sometimes even mylonitic rocks. Within large parts of the intrusive, the orthoclase megacrysts are recrystallized and transformed into mixed crystalline aggregates with components of intermediate microcline, where the proportion of microcline component is increased by the degree of deformation. However, in other deformed parts of the intrusive, the orthoclase is stable and the K-feldspar megacrysts may appear as fractured, surrounded by fine grained recrystallized domains of quartz, plagioclase and myrmekite. The different appearance of the K-feldspar megacrysts associated with deformation suggests an early event of deformation where orthoclase was stable, at high T-conditions, followed by a later deformational phase in which orthoclase was transformed into a mixed crystalline state with components of intermediate microcline. Furthermore, rocks with stable orthoclase appear homogeneously foliated whereas rocks that display a distinct structural change within the K-feldspar megacrysts mainly occur as discrete deformation zones.

Zircons from an undeformed pegmatitic dyke, intersecting the gneissosity in a strongly deformed part of the granite, yield an age of ca. 955 Ma by Pb-Pb evaporation. This age is the minimum age of the regional deformation that affected the Tjärnesjö massif. The maximum age is set by the ca. 1.36 Ga intrusion age of the granite massif .

The granulite facies mineral assemblages present in the charnockitoids define a high grade foliation at deformed sites. This high-grade event is interpreted to be late Sveconorwegian.

Jenny Andersson
Geologiska Institutionen
Avd. för Mineralogi & Petrologi
Sölvegatan 13, S-223 62 Lund, Sweden

Contents: Page:

1. Introduction

1.1 Overview

Late Sveconorwegian deformation and granulite facies metamorphism in southwestern Sweden have been described by several previous authors (Johansson et al. 1991; Johansson & Kullerud 1993; Johansson & Johansson 1993; Wang & Lindh in press; Möller & Söderlund submitted). The extension and importance of the Sveconorwegian event in the region is still uncertain. The occurrence of charnockite massifs is typically associated with granulite facies terrains and several charnockites have consequently been discovered within the Southwest Swedish Granulite Province (SGP). The most well known of them is the Varberg Charnockite Granite Association, (CGA), which has been described by several previous authors (e.g. Quensel 1950; Hubbard 1975, 1978, 1989; Hubbard & Whitley 1979; Gaàl & Gorbatschev 1987; Talbot & Heeroma 1989; Åhäll et al. 1992; Johansson & Kullerud, 1993). However, several minor occurrences of charnockitic rocks have been reported from the SGP, mainly along the well exposed coastline (Johansson & Kullerud 1993). These occurrences generally appear as lenses or as diffuse patches in high grade gneisses and sometimes in granitoids.

1.2 Charnockites

The origin of charnockites has been the subject of intense discussion. The "original" charnockite was a hypersthene-bearing granitic rock, found in the tombstone of Job Charnock, the founder of Calcutta (Holland 1900). According to the recommendations of the IUGS (Le Maitre 1989), the term charnockite should be used only to describe hypersthene-bearing, granular rocks of a granitic composition. However, the term charnockite has in practise been used for hypersthene-bearing rocks ranging in composition from granites and intermediate igneous rocks, to mafic rocks like norites and anorthosites. Such hypersthene-bearing, non-granitic rocks have a nomenclature of their own (Le Maitre 1989). Although charnockites of a sedimentary origin, i.e. hypersthene-bearing paragneisses, have been reported from several localities throughout the continents, the QAP plot for igneous rocks (Streckeisen 1974, 1976) is used for the classification of all charnockites irrespective of their origin. The granite massif at Tjärnesjö described in this investigation is associated with quartz-monzonitic pyroxene-bearing units. However, the pyroxene bearing rocks in the Tjärnesjö intrusive contain no hypersthene, and the term charnockitoid is used here to avoid confusion with the definition of charnockite described above.

Charnockites described in the literature include a wide range of rock types. They differ from each other in origin as well as in the way the charnockitization process has affected the rock. However, irrespective of the genetical background of the rock, the occurrence of charnockite is generally restricted to granulite-facies areas. The general idea of the formation of charnockites is that they evolve either due to *in situ* metamorphism, or as primary crystallization products of an originally dry magma.

Metamorphic charnockites are usually found among high-grade gneisses and a common theory of the formation of such rocks is that they are transformed into a charnockitic state by the influx of CO_2-rich fluids, resulting in the dehydration of the present mineral assemblage. This process is considered to take place at upper amphibolite or granulite facies metamorphic conditions, at low P_{H2O} (Janardhan et al. 1979; Allen et al. 1984; Burton & O´Nions 1990; Yoshida et al. 1991; Andersson et al. 1992; Perchuk & Gerya 1993).

Intrusive charnockites are believed to originate from the primary crystallization of a hypersthene-normative, dry magma. According to the general theory of the petrogenesis of such rocks, they intrude as primary dehydrated restite melts, and they are generally associated with a differentiated granitoid magmatic suit (Petersen 1980; Hubbard 1989; Kilpatrick & Ellis 1992; Dada et al. 1995). According to Kilpatrick & Ellis (1992) the igneous charnockites define a distinctive magma type, the Charnockite Magma Type, CMT or C-type magma, differing in chemical bulk composition from the established I, S and A-type magmas and the metamorphic charnockites. However, an originally hypersthene-bearing, charnockitic magma is hard to demonstrate, since these rocks commonly occur in high-grade terrains, where the present mineral assemblages most likely have been affected by post-magmatic high P-T deformation and metamorphism.

It is very important to differentiate between magmatic and metamorphic charnockites since metamorphic charnockites reflect a regional high-grade metamorphism at granulite or upper amphibolite facies conditions (Newton et al. 1980; Yoshida et al. 1991; Perchuk & Gerya 1993, and references cited in these sources.).

While rocks of granitoid composition often contain zircons - in contrast to mafic granulites were zircons are rare - metamorphic charnockites should be easier to date and still contain the high-grade mineral assemblages required for interpretation of the metamorphism.

1.3. Purpose of the study

The investigation of the Tjärnesjö massif was restricted to the southern parts of the area, where the occurrence of pyroxene-bearing granitoids had been reported. Since this study mainly focuses on the influence of Sveconorwegian metamorphism and deformation of the present granitoids, no attempt at petrogenetic modelling is made. The petrological character of the Tjärnesjö granitoids was investigated by studies of thin sections and complemented by electron microprobe EDX analyses. Age determinations were carried out in order to date the intrusion of the Tjärnesjö massif and thereby constrain the maximum age for metamorphism and deformation of the granitoids. An undeformed pegmatitic dyke, located in the granite body, was also dated. The dyke cross-cuts a ductile deformation zone, and the emplacement age of the dyke consequently sets a minimum age of the deformation. Chemical analyses were made to classify the granitoids, and together with age determinations, to correlate the Tjärnesjö massif with the Varberg Charnockite Granite Association (CGA) further to the west. Field studies were carried out in order to map the extension of the pyroxene-bearing units, and to study the degree and extent of the deformation that affected the Tjärnesjö massif.

2. Geological setting

2.1 A regional overview

The Precambrian in southwestern Sweden consists mainly of post-Svecofennian rocks, approximately between 1750-1200 Ma old. The region is characterized by extensive reworking of the country rocks, during the Sveconorwegian orogenic event ca. 1200-900 Ma ago. Although only a little new crustal material was added to the province during this period, it resulted in a widespread tectonic and metamorphic processing of the preexisting crust (Gaàl & Gorbatschev 1987). The southwestern part of the Baltic Shield in Sweden is divided by two major shear zones, in the east by the Protogine zone (PZ) and the Sveconorwegian Frontal Deformation Zone (SFDZ), and in the northwest by the Mylonite zone (MZ) (Fig 1). These boundaries mark significant breaks in the degree of deformation and metamorphism. The southern part of the region, the Southwest Swedish Granulite Province (SGP), is characterized by the abundance of granulite-facies rocks. It is mainly composed of strongly deformed, high-grade, veined to sometimes migmatitic gneisses, intruded by granitoid and mafic rocks. The north-southerly extension of this high-grade domain is not well defined, but granulitic rocks have been reported from Skåne in the south, to the areas of Ulricehamn and Borås in the north (Johansson et al. 1991) (Fig 1). P-T estimates from several granulite sites within the region display pressures around 8-10.5 kbar and temperatures around 665-800° C (Johansson et.al. 1991; Johansson & Kullerud 1993; Wang & Lindh in press). Datings of metamorphic mineral assemblages on rocks from the SGP give late Sveconorwegian ages (Johansson et al. 1991; Johansson & Kullerud 1993; Söderlund in press; Wang et al. in prep.; Page et al. in prep.).

The Varberg Charnockite Granite Association, which is the largest occurrence of charnockites in the SGP, consists of several different charnockite units and associated granitoids. Hubbard and Whitely (1979) described the charnockites at Varberg as two-pyroxene-bearing, massive, granular rocks, with distinctively dark-coloured quartz and feldspar, displaying a compositional differentiation from tonalite to granite. In later work, Hubbard (1989) suggested a close genetic relationship between the different units of the CGA. He proposed a petrogenetic model, whereby the complex develops by segregation of magmatic components, with the Torpa granite intruding at a higher crustal level, leaving the differentiated, dehydrated, charnockitic restites at the base of a rising melt-plume. According to Hubbard (1989, and references therein), both igneous and metamorphic processes were involved in the charnockite forming processes in the Varberg CGA.

2.2 Geological setting of the Tjärnesjö granite

The investigated area is located in the western parts of the Southwest Swedish Granulite Province which constitutes the southern parts of the Eastern segment (Fig. 2). It comprises highly deformed and metamorphosed, veined and locally migmatitic fine-grained gneisses, intruded by mafic and granitoid rocks. The gneisses range in composition from reddish and greyish felsic rocks to intermediate or mafic, greyish rocks. They are of unknown age and origin, however, most likely older than the granitoids described in this study.

The Tjärnesjö massif is dominated by a coarse-grained, megacrystic orthoclase granite. It forms an approximately north-southerly narrow, elongated body, about 30 km. long. While the fine-grained adjacent gneisses are strongly deformed, veined and in places migmatitic, the coarse-grained megacrystic granite body appears more well preserved, though zones of intense deformation are common throughout the massif.

Of major interest in the investigated area is the occurrence of pyroxene-bearing, quartz-monzonitic rocks, here referred to as charnockitoids. These rocks are mainly present in the internal parts of the massif (Fig. 3), and they are readily distinguished from the true granite by their typical brownish colour. Fine-grained xenoliths are common in the charnockitoids. The xenoliths are often deformed and elongated concordant with the foliation in the host rock. The true granites occasionally contain xenoliths but to a lesser extent.

"Aplitic" dykes are often observed in the granitoids. The term aplitic is used here to define a fine-grained rock of approximately the same composition as the host rock. Aplites occur both as thin dykes, generally a few cm. across, or sometimes as larger units. Both aplites and granitoids are foliated, but the foliation of minor dykes may sometimes appear discordant with the gneissosity in the host rock. This apparent discordance is however due to refraction of the foliation, where finer grained units have responded differently to the deformation than the coarser grained host rock.

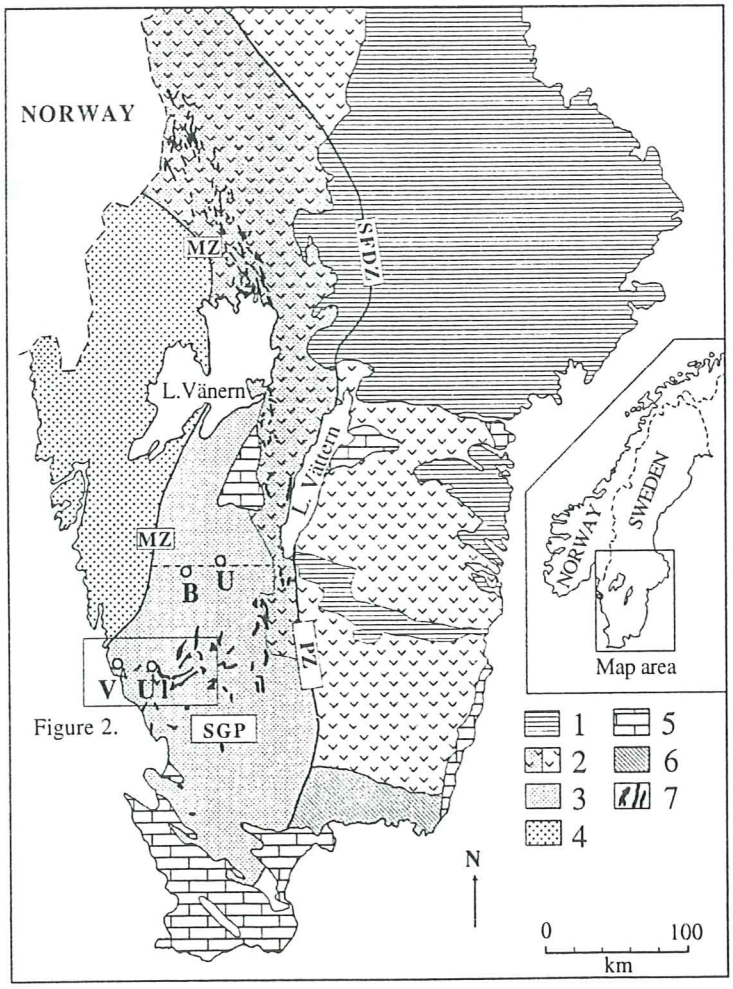

Fig. 1. Geological map of Southern Sweden. (Modified after Wahlgren et al. (1994) and Söderlund (in press).) Major geological provinces: (1) Svecofennian Province; (2) Trans-scandinavian Granite-Porphyry Belt; (3) Eastern segment of the Southwest Swedish Gneiss Province, where the southern part constitutes the South Swedish Granulite Province (SGP). The approximate northern extension of the SGP is marked by the dashed line through U and B; (4) Western segment of the Southwest Swedish Gneiss Province; (5) Neoproterozoic and Phanerozoic cover; (6) Blekinge Province; (7) Mafic and metamafic rocks as dykes, lenses, or as larger intrusions.
Major Tectonic boundaries: MZ=Mylonite Zone, PZ=Protogine Zone, SFDZ=Sveconorwegian Frontal Deformation Zone,
B=Borås, U=Ulricehamn,
Ul=Ullared, V=Varberg

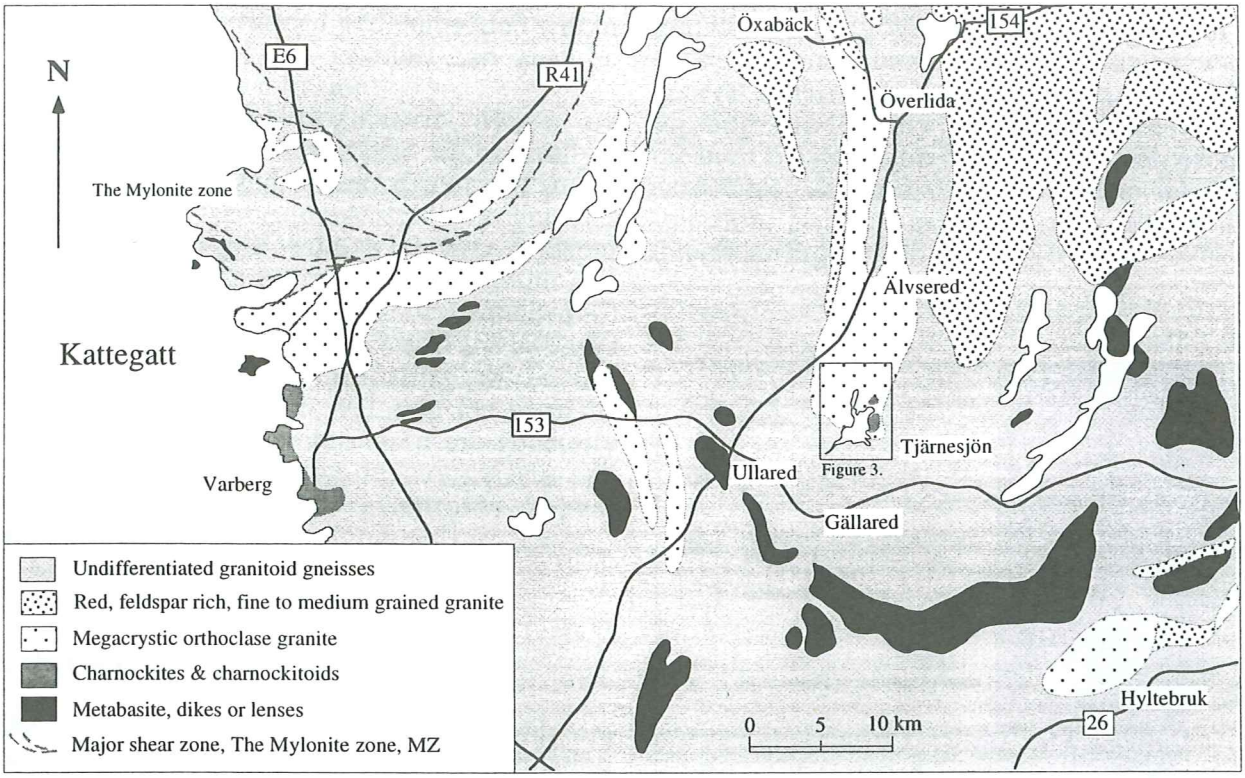

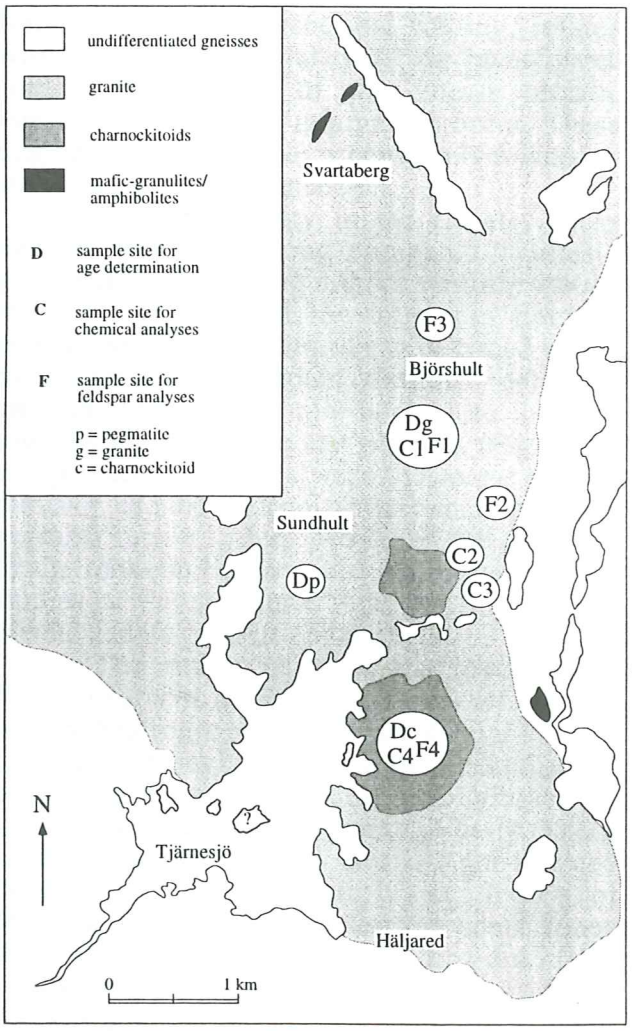

Above, Fig. 2. Regional geological map of a part of the Eastern segment of the Southwest Swedish Gneiss Province (SGP). (Modified after Provisoriska Översiktliga Berggrundskartan (PÖB), Sveriges Geologiska Undersökning (SGU), Ser Ba no 41, Borås)

Left, Fig. 3. Geological map of the southern regions of the Tjärnesjö intrusion.

Several high-grade mafic bodies occur in the region. P-T estimates from the Ullared granulite, situated approximately 15 km. southwest of the Tjärnesjö intrusive, yield pressures around 10.5 kbar and temperatures of ca. 770° C. Sm/Nd mineral dating from the same site gives an age of ca. 916 ± 11 Ma (Johansson et al. 1991). This age was originally interpreted to date the peak of the granulite facies metamorphic event in the area. However, recent data from U/Pb dating (Söderlund, in press; Wang et al. in prep.) and Ar/Ar dating on hornblende (Page et al. in prep.) of Sveconorwegian deformation and metamorphism in the region give considerably older ages, and the ca. 916 Ma age of the Ullared mafic granulite is therefore to be considered as a strict cooling age of the Sm/Nd system of the rock.

In the northern parts of the investigated area, mafic dykes, which have undergone granulite facies metamorphism, occur within the

granite massif (Fig. 3). Amphibolitized mafic dykes, strongly deformed and embedded within the gneissosity of the granite, can also be observed within the intrusion.

Undeformed pegmatitic dykes are common in the area. The dykes are generally a few meters wide and appear discordant to the foliation in the Tjärnesjö massif. The pegmatites are typically light reddish, quartz-feldspar dominated, with minor amounts of biotite and sometimes magnetite. Minor concordant pegmatitic mobilisates such as veins and enclaves may also be present indicating an *in situ* mobilization. Pegmatitic veins in the gneisses that surrounds the granite massif are generally penetratively foliated, while mobilisates and veins in the Tjärnesjö granitoids appear undeformed.

3. Structures

The area where the Tjärnesjö granitoids are located is characterized by strong deformation and reworking of the country rocks. Generally the surrounding gneisses are penetratively foliated, displaying isoclinal folding, rotated within the foliation planes. In the investigated southwestern parts of the gneiss terrain, intermediate to mafic migmatites occur. These migmatitic rocks are not penetratively foliated as are the adjacent felsic gneisses.

The gneissosity in the country rocks sweeps around the long elongated Tjärnesjö granite massif, forming a large synform around the southern parts of the intrusion. Locally, similar synformal structures can be traced within the granite, and the amount of strongly deformed gneissic Tjärnesjö granite appears to increase towards the contact to the gneisses (Fig. 4). A competence contrast between the coarse grained intrusion and the adjacent country rocks probably explains such a feature. However, the exposure of the rocks in the area did not allow detailed studies of the structural relations between the granite and its gneissic environment.

The major parts of the investigated Tjärnesjö granite are foliated, but the deformation is very heterogeneous and varies from slightly foliated to strongly foliated rock. Local discrete deformation zones occur throughout the investigated parts of the granitoid body. These zones are sometimes very strongly gneissic and in places even mylonitic. The degree of deformation within such discrete shear zones may vary rapidly within only a few dm., from almost massive granite to strongly foliated, gneissic granite. No general direction of these zones is observed. On the contrary, parts of the granite, typically within the central parts of the massif, are more homogeneously foliated, with a general foliation in a north-westward direction, dipping moderately to the northeast. This includes the pyroxene-bearing quartz-monzonitic associates, which display a slight to moderate foliation, striking generally in a N60W/45N direction (Fig. 4).

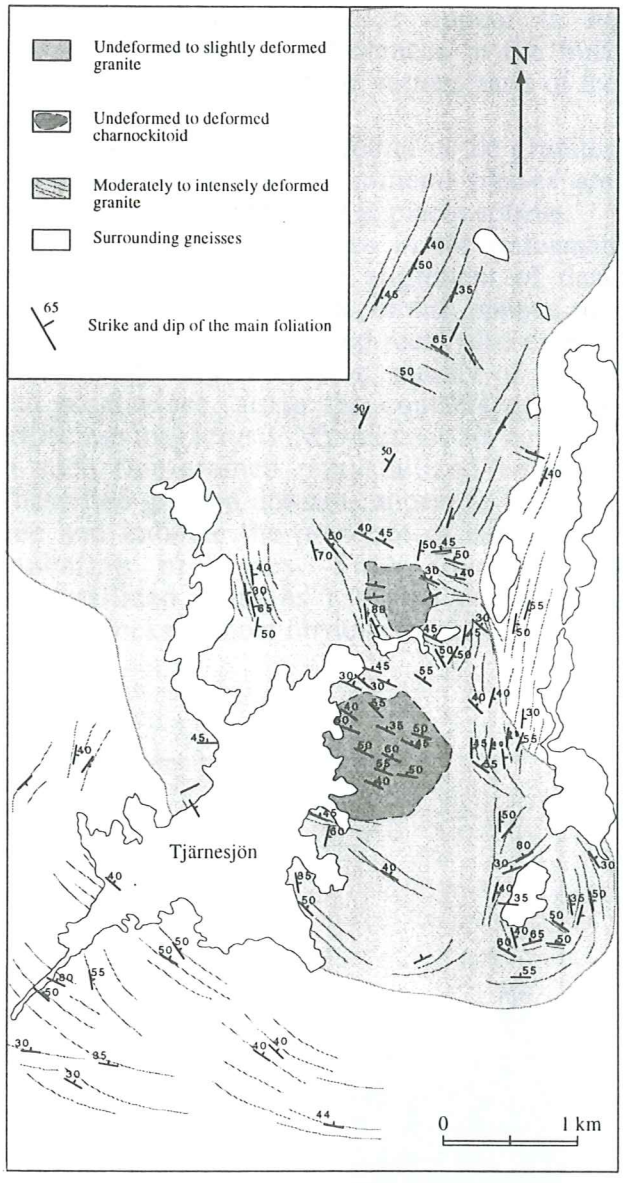

Fig. 4. Structural sketch map of the southern parts of the Tjärnesjö region. The gneissosity in the adjacent gneisses forms a large synform around the southern parts of the granite intrusion. Note that similar synformal structures can be traced within the granite towards the contact with the surrounding gneisses.

4. Petrology and petrography

4.1 The Tjärnesjö granite

The Tjärnesjö granite is a coarse grained, reddish to greyish, megacrystic orthoclase granite. Orthoclase megacrysts from massive to slightly foliated granite are perthitic, commonly microperthitic, with fine blebs of embedded plagioclase (Fig. 5). The anorthite-component in plagioclase varies between An_{15} and An_{25} (Fig. 6). Plagioclase inclusions found in perthitic K-feldspar crystals have the same anorthite content as the matrix plagioclase. In recrystallized sericitised crystals, the anorthite component is lower, around An_{05} (Fig 6, plagioclase analyse no. 8 & 9). The degree of sericitisation varies between different parts of the granite.

Among the Fe-Mg minerals ferroan-pargasitic hornblende (Fig. 7) is the most common mineral. The hornblende is greenish, poikiloblastic, often rich in inclusions of quartz and opaques. Biotite is brown to reddish-brown and in places present as a late phase, where it mainly replaces hornblende during retrogression.

The granite sometimes contains metamorphic garnet, the amount of which varies widely between the different granitic units. The garnets are generally anhedral and poikiloblastic. A rim of plagioclase often occurs between the anhedral garnet and hornblende, which suggests reequilibration during retrogression. Less retrograded grains occur in textural equilibrium with hornblende. Garnet commonly occurs as small grains, forming coronas around dark mineral aggregates, typically composed of hornblende or opaques. In places they also occur as single, small homogeneous, non-poikiloblastic grains. The ability to form garnet during the high grade event that affected the granitoids appear to be controlled mainly by differences in the bulk chemical composition of the various parts of the massif.

No pyroxenes are found in the granites *sensu strictu*. Accessory mineral phases are opaques, zircon apatite, and in places sphene.

The foliation planes in the deformed rocks are defined by the alignment of dark minerals such as hornblende, biotite, opaque and sometimes garnet. Deformed rocks also display widespread recrystallization, mainly of quartz and plagioclase, along the contacts of large orthoclase megacrysts. Myrmekites are common in such fine-grained recrystallized volumes. These fine grained domains appear to be strain free and indicate the presence of subsequent annealing processes. Such fine grained recrystallized domains are also common in massive rocks without obvious foliation.

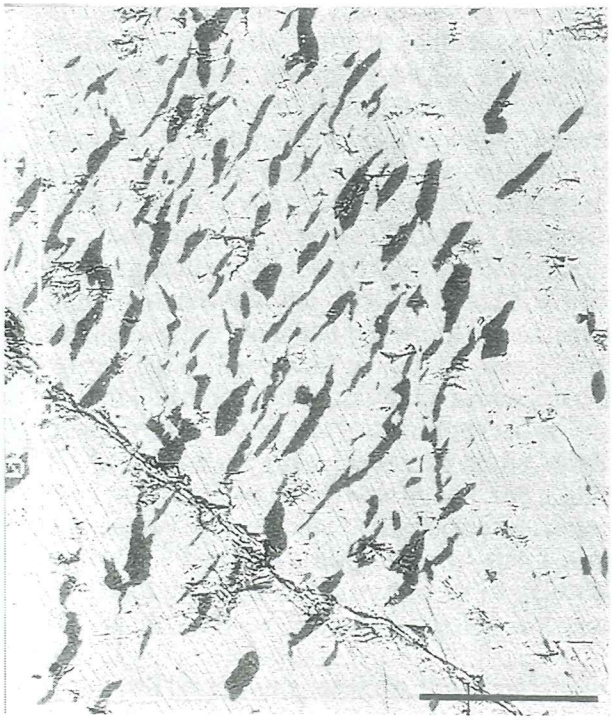

Fig. 5. Perthitic feldspar from granite C1. Length of scale is ca. 100 µm.

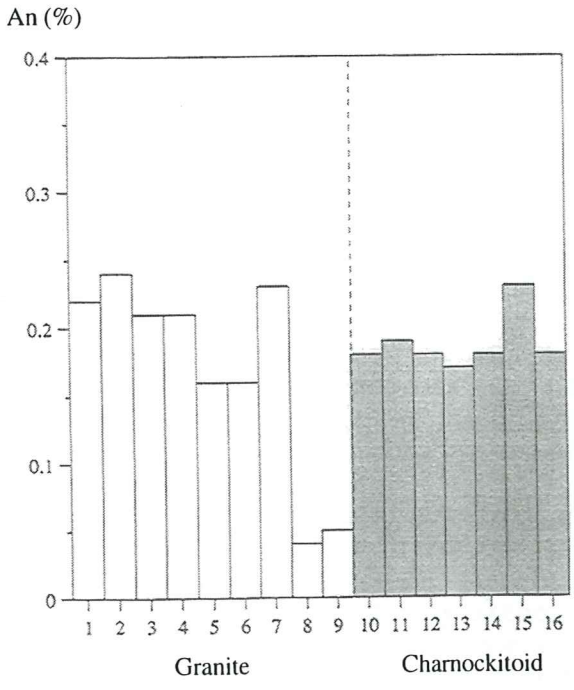

Fig. 6. Anorthite component in plagioclase. Open staples=granite, C1; Filled staples=charnockitoid, C4.

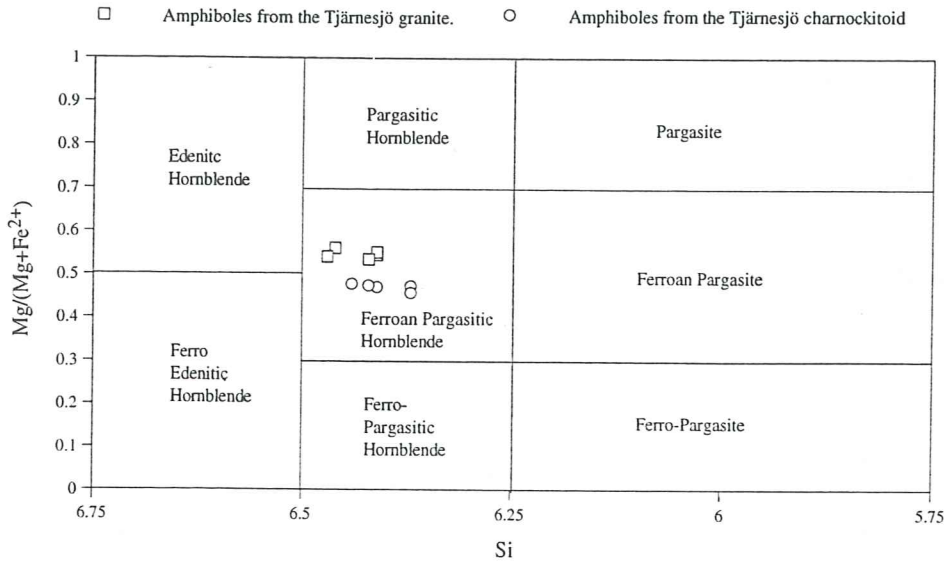

Fig. 7. Classification of Calcic-Amphiboles from the Tjärnesjö granitoids according to Leake (1978). Squares = granite, circles = charnockitoid.

4.2 The Tjärnesjö charnockitoid

In the central parts of the investigated area of the granite massif, several outcrops of an earlier unknown clinopyroxene-bearing rock, here referred to as charnockitoid, were discovered. The charnockitoid is a medium-grained brownish rock. Large megacrysts of K-feldspar occur, though they are less common than in the granite. The difference between the pyroxene-bearing charnockitoid and the granite is readily observed in field due to the dark brownish colouring of particularly the feldspars in the charnockitoid rocks. Investigations of metamorphic charnockite gneisses at Kabbaldurga, south India (Janardhan et al. 1979), showed that the colouring of these rocks was related to the presence of submicroscopic veins of chlorite and manganese-bearing calcite especially in the feldspars. He demonstrated that the dark-coloured charnockite gneisses were bleached when put in contact with warm HCl. This was tested on the Tjärnesjö charnockitoids, and most of the brownish colour disappeared when rock specimen were put in HCl (25%) for approximately 24 hours. After the acid treatment, the rock was lighter and similar in appearance to weathered charnockitoids observed in field. The brown colouring of the Tjärnesjö charnockitoids is suggested to be largely due to the occurrence of Fe-oxides hosted in fractures and along grain boundaries.

The K-feldspar is perthitic and in places displays Carlsbader twinning. X-ray diffraction analysis of the K-feldspar shows no microclinization in the orthoclase, although the rock examined is clearly foliated (cf. Section 5. Deformation and feldspar mineralogy). Perthitic K-feldspar of the charnockitoids hosts larger plagioclase inclusions than the perthites in the granite. The anorthite content ranges between An_{15} and An_{20} (Fig. 6). Analyses from larger plagioclase inclusions in perthite give a somewhat higher anorthite content of An_{25} (Fig. 6, plagioclase analyse no. 15). Along grain boundaries of coarse feldspar grains, fine-grained domains occur, consisting mainly of recrystallized quartz, plagioclase and commonly also myrmekite. Recrystallized domains, containing myrmekite, are also a common feature in rather massif charnockitic rocks.

The amphibole in the charnockitoid is a ferroan pargasitic hornblende, with only a somewhat lower $Mg/(Mg+Fe^{2+})$ ratio than the amphibole in the granite (Fig. 7). The amphiboles are green to light green in colour, and they generally dominate the dark mineral phases. Hornblende appears as nearly homogeneous crystals or as partly altered, anhedral grains, where inclusions, mainly of quartz, are common.

All pyroxene-bearing granitoids in the investigated area are referred to as charnockitoids. The pyroxene present is a ferrosalitic-ferroaugitic clinopyroxene, with approximately equal molar proportions of $CaFeSi_2O_6$ and $CaMgSi_2O_6$, (Fig. 8; Tab. 1). Large crystals are altered and appear in various stages of retrogression, primarily to amphibole and chlorite but also possibly to other sheet

silicates. The large grains are also characterized by the occurrence of distinct exsolution lamellae, common for magmatic pyroxenes. Pyroxene neoblasts are far less retrograded or completely unaltered and exsolution lamellae are absent in such small clear grains. In larger aplitic occurrences, well preserved clinopyroxene is very common, while pyroxene is absent in some deformed minor aplitic dykes. Pyroxenes in the aplites do not differ in composition from pyroxenes in the medium-grained parts of the charnockitoids.

Garnet is common in all charnockitoid samples. The garnets typically appear as fine grained coronas, growing around the dark mineral phases, such as hornblende, clinopyroxene and opaque. Large, single grains are typically poikiloblastic, while smaller grains are generally more well preserved and may be almost idioblastic. Garnets analysed by electron microprobe reveal an overall uniform garnet composition of Prp_{7-9} Alm_{65-67} Grs_{19-20} Sps_{6-7} (Tab. 2). According to Sobolev (1965) and Wedding (1987), a high grossular- and a low spessartine-component indicate a metamorphic garnet. Electron images displayed garnet and pyroxene in textural equilibrium (Fig. 9).

Biotite is typically brown to reddish brown. In places it appears as a late mineral, growing at the expense of particularly hornblende and pyroxene. Accessory minerals are mainly zircon, opaque and apatite.

The foliation planes in deformed charnockitoid rocks are defined by the alignment of dark phase minerals such as clinopyroxene, hornblende and garnet. The distribution of these minerals are described above. In view of the mineral assemblages associated with the deformation, the present foliation is clearly high-grade in character. The gneissic discrete deformation zones associated with microclinization of the K-feldspar present in the granite have not been observed within the charnockitoid parts of the intrusion.

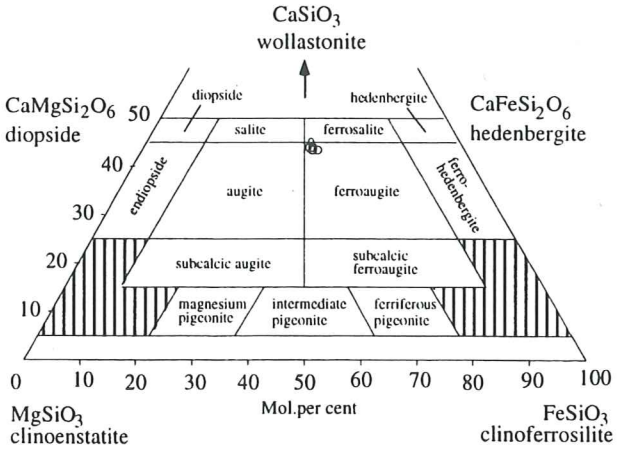

Fig. 8. Classification of pyroxenes from the Tjärnesjö charnockitoid C4, after Deer et al. (1987).

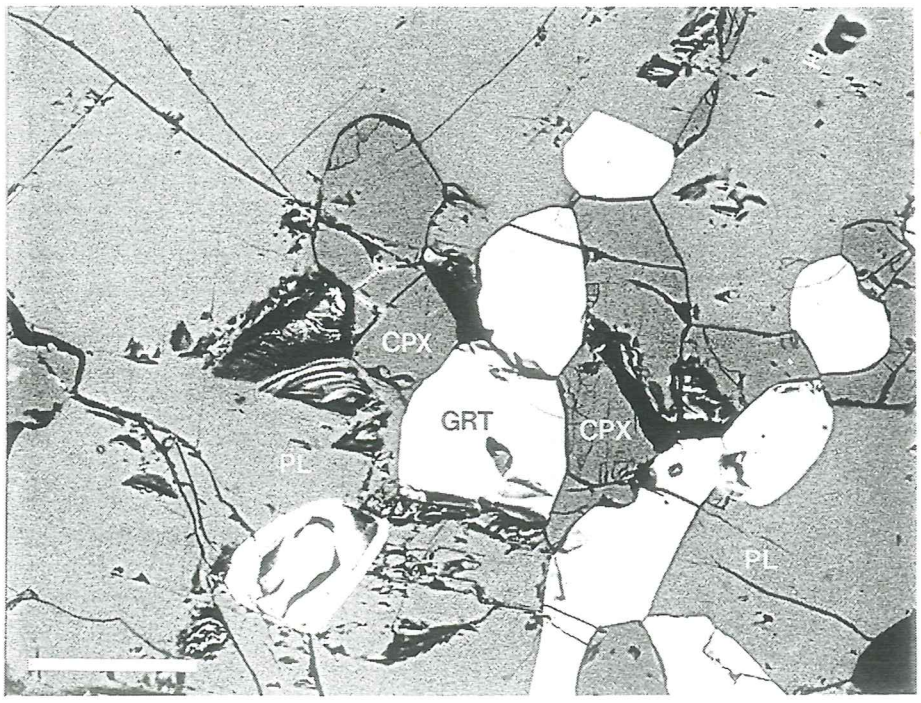

Fig. 9. Garnet (GRT) and clinopyroxene (CPX) in textural equilibrium, from the Tjärnesjö charnockitoid C4, (PL=plagioclase). Length of scale is ca. 100 μm.

Tab. 1. Chemical composition of pyroxenes from the Tjärnesjö charnockitoid (sample-site C4). Cation formula is based on six oxygen atoms.

Oxides (wt%):	P1	P2	P3	P4	P5	P6
Na_2O	0.78	0.97	0.61	0.83	0.62	0.73
MgO	8.81	8.79	9.08	8.93	8.93	9.01
Al_2O_3	1.65	1.85	1.39	1.68	1.55	1.24
SiO_2	50.22	50.60	51.22	51.07	50.96	50.68
CaO	20.39	21.04	20.57	20.30	20.39	20.85
MnO	0.43	0.40	0.40	0.54	0.48	0.48
$FeO+Fe_2O_3$	16.59	15.94	17.01	16.94	16.81	16.38
Total:	98.87	99.59	100.28	100.29	99.74	99.37
Cations:	P1	P2	P3	P4	P5	P6
Na^+	0.06	0.07	0.05	0.06	0.05	0.05
Ca^{2+}	0.85	0.87	0.85	0.84	0.85	0.87
Mn^{2+-4+}	0.01	0.01	0.01	0.02	0.02	0.02
Mg^{2+}	0.51	0.51	0.52	0.51	0.52	0.52
Fe^{2+}-Fe^{3+}	0.54	0.52	0.55	0.55	0.54	0.53
Total:	1.97	1.98	1.98	1.98	1.98	1.99
Al^{3+}	0.08	0.08	0.06	0.08	0.07	0.09
Si^{4+}	1.96	1.96	1.97	1.97	1.97	1.97
Total:	2.04	2.04	2.03	2.05	2.04	2.06
Endmembers (%):	P1	P2	P3	P4	P5	P6
Clinoenstatit	27	27	27	27	27	27
Clinoferrosilit	28	27	29	29	28	28
Wollastonite	45	46	44	44	45	45
Total:	100	100	100	100	100	100

Tab. 2. Chemical composition of garnets from the Tjärnesjö charnockitoid (sample-site C4). Cation formula is based on 12 oxygen atoms.

Oxides (wt%):	Gt 1	Gt 2	Gt 3	Gt 4	Gt 5
$FeO+Fe_2O_3$	30.99	31.48	31.01	31.11	30.83
CaO	7.00	7.13	6.90	6.88	6.95
MgO	2.23	2.00	1.85	1.97	1.80
MnO	2.85	2.86	3.01	3.09	3.37
Al_2O_3	20.70	20.32	20.42	20.62	20.39
SiO_2	37.25	37.04	37.18	36.94	36.58
Total:	101.02	100.83	100.37	100.61	99.92
Cations (M1,M2):	Gt 1	Gt 2	Gt 3	Gt 4	Gt 5
$Fe^{2+}+Fe^{3+}$	2.07	2.11	2.09	2.09	2.09
Ca^{2+}	0.60	0.61	0.59	0.59	0.60
Mg^{2+}	0.27	0.24	0.22	0.24	0.22
Mn^{2+-4+}	0.19	0.19	0.21	0.21	0.23
Total:	3.13	3.15	3.11	3.13	3.14
Cations (X,Y):	Gt 1	Gt 2	Gt 3	Gt 4	Gt 5
Al^{3+}	1.95	1.92	1.94	1.95	1.95
Si^{4+}	2.97	2.93	2.99	2.97	2.96
Total :	4.92	4.85	4.93	4.92	4.91
Endmembers (%):	Gt 1	Gt 2	Gt 3	Gt 4	Gt 5
Almandin	65	66	67	66	66
Grossular	20	20	19	19	20
Pyrop	9	8	7	8	7
Spessartin	6	6	7	7	7
Total:	100	100	100	100	100

5. Deformation and feldspar mineralogy

5.1 Overview

Deformed parts within the granite intrusive often display transformation of the orthoclase megacrysts into mixed crystalline states with components of intermediate microcline. The structural conversion of K-feldspar seems to increase with the degree of deformation, although "microclinization" may be observed also in gently foliated parts. The conversion of the orthoclase can be observed in field, where the orthoclase megacrysts of reddish-greyish colour in massif rocks develop reddish discrete zones of intermediate microcline, up to ca. 1mm wide, at moderate deformation, then turning into fine grained aggregates of reddish microcline when strongly deformed. However, even in intensely deformed zones, remnants of orthoclase megacrysts can be found in the fine-grained, microcline aggregates. In protomylonites, orthoclase is absent and are replaced by fine-grained microcline aggregates, of approximately the same size as an average Tjärnesjö granite orthoclase megacryst (Fig. 10 a-d).

However, homogeneously foliated rocks generally located in the central parts of the intrusion, do not have "microclinized" orthoclases. Instead, large orthoclase megacrysts in places appear fractured, surrounded by fine grained recrystallized quartz, plagioclase and myrmekite. Fracturing of large K-feldspar megacrysts at ductile deformation have been described by Srivastava & Mitra (1996) and Michibayashi (1996). According to these authors, the presence of a weak, fine-grained matrix (e.g. a fine-grained matrix of plagioclase and quartz) plays an important role for the development of the stressfield in the megacryst. The same authors point out that the amount of fractures is increased with the size of the crystal.

5.2 K-feldspar analyses

MacKenzie (1954) demonstrated that the crystallographic nature (triclinicity) of K-feldspar could be determined by the spacing of the reflections from the 131 and $1\bar{3}1$ lattice planes. If only a single 131-peak reflection is present, the feldspar is a monoclinic Al disordered feldspar (orthoclase/sanidine) (Fig 11a). A broadened, diffuse, separated reflection indicates the presence of an intermediate microcline phase,

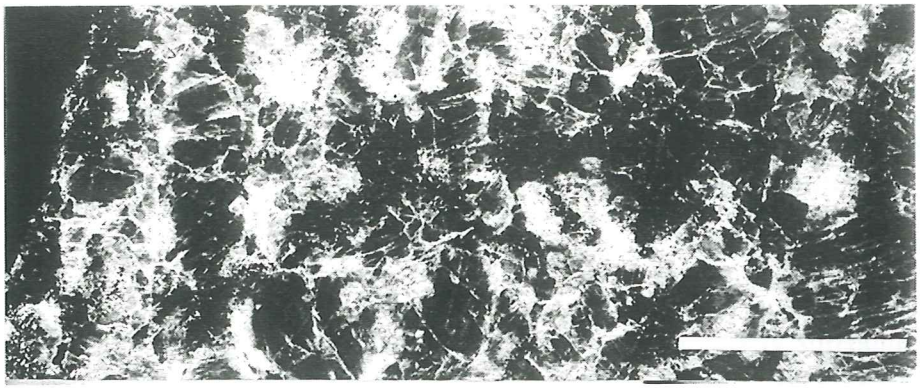

Fig. 10 a-d. Four samples from the Tjärnesjö granite, in various stages of deformation. Length of scale is ca. 2 cm:

(a) A massive part of the granite, sample F1, where the orthoclase megacrysts are almost intact.

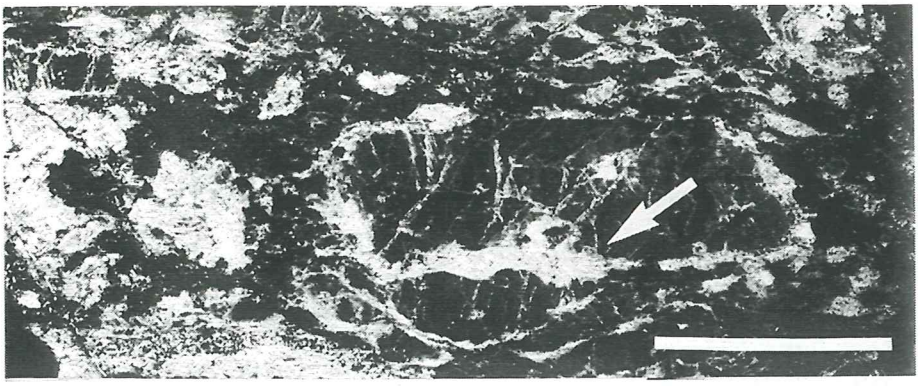

(b) A slightly deformed part of the granite, sample F2, displaying a beginning conversion of the orthoclase. Fine-grained domains of quartz, myrmekite and plagioclase are developed along the boundaries to large K-feldspar megacrysts.

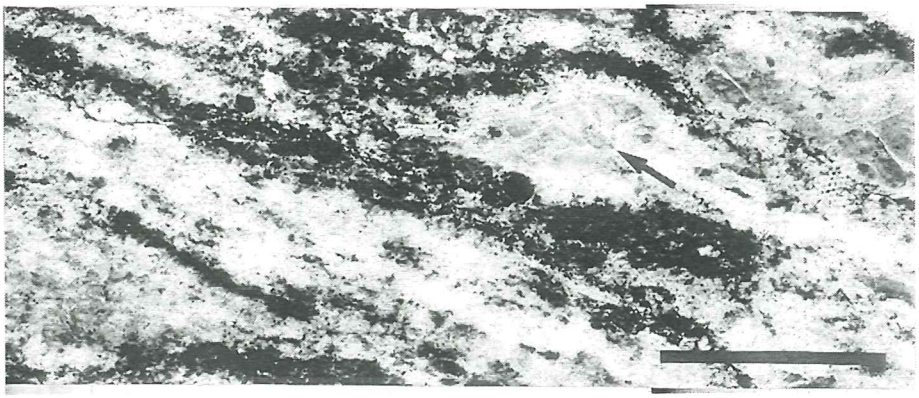

(c) An intensely deformed part of the granite, sample F3, where the large orthoclase megacrysts are transformed into fine-grained aggregates dominated by microcline. Remnants of orthoclase augens can still be observed.

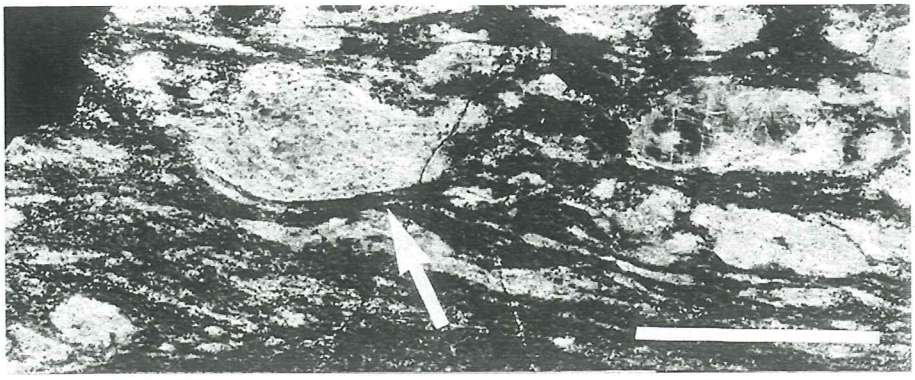

(d) A transition zone to a protomylonitic part of the granite. The orthoclase megacrysts are replaced by fine-grained aggregates of microcline of approximately the same size as an average orthoclase megacryst in the Tjärnesjö granite.

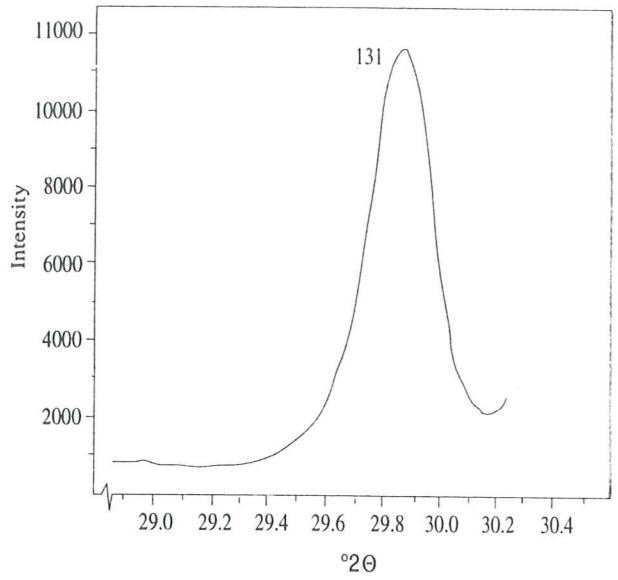

Fig. 11 a

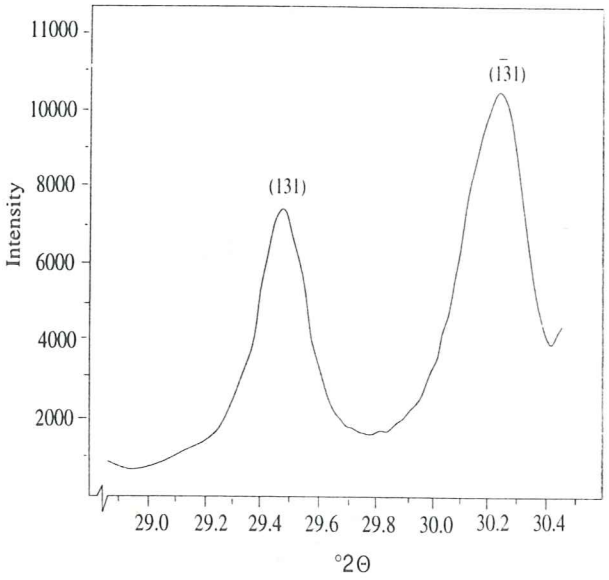

Fig. 11 b

Fig. 11. X-ray diffractogram from K-feldspar analyses, modified after Mannerstrand (1992).
(a) Monoclinic K-feldspar - orthoclase , from the Apelviken-Getterön charnockites, Varberg; **(b)** Triclinic K-feldspar - microcline, from a pegmatite.

while a triclinic feldspar (microcline) displays two distinct, 131 and $1\bar{3}1$, well separated peaks (Fig. 11b). For a more detailed description of the method for discriminating between monoclinic and triclinic K-feldspar, see MacKenzie (1954), Goldsmith & Laves(1954) and Mannerstrand (1992).

K-feldspar megacrysts from the Tjärnesjö granitoids were analysed by X-ray diffraction, in order to examine the crystallographic character of the K-feldspar. Three different samples from the granite, F1-F3, and one from the charnockitoid, F4, were examined For location of sample-sites, see Fig. 3. Sample F1 comes from a massive, coarse grained granite (Fig. 10 a). The second sample, F2, was taken from a slightly foliated granite, where the large orthoclase grains exhibit a reddish component along discrete zones up to ca. 1 mm wide. These large megacrysts are commonly surrounded by a fine-grained matrix of quartz, plagioclase and myrmekite (Fig. 10 b). Sample F3 comes from an intensely deformed shear zone in the granite, where the K-feldspar megacrysts appear to be almost entirely transformed into reddish fine-grained aggregates of microcline. Remnants of K-feldspar megacrysts occur sparsely in the fine grained aggregates (Fig. 10 c). Sample F4 was taken from a foliated part of the charnockitoid, where no conversion of the orthoclase phase was observed in field.

The crystals were handpicked from crushed samples, and ground to a fine powder in a mortar. Approximately five grams were taken from each specimen for the preparation of powder pellets. All analyses were made in a Philips X-ray diffractometer PW 1710, with monochromatic CuK_α radiation (λ=1.5418 Å, 50 kV, 25 mA).

5.3 Results

The massive parts of the Tjärnesjö granite, sample F1, yield a single 131-peak, (although somewhat broadened) (Fig. 12a), though a dominance of the orthoclase phase is evident. K-feldspar from slightly deformed granite, sample F2, displays a more broadened 131-peak, still without any distinct separation of the peak reflection (Fig. 12b). Consequently, the feldspar phase in sample F2 is mainly monoclinic, though the slight broadening of the reflex suggests the presence of a triclinic component. Finally, K-feldspar from the deformation zone at sample site F3 displays a significant broadening of the reflex, where a defined 131-peak is absent. This clearly indicates the increased presence of an intermediate microcline component (Fig. 12c). In contrast, the feldspar sample from the foliated charnockitoid, sample F4, shows the most well defined 131-peak (Fig. 12d) of the samples analysed, comparable to an almost pure monoclinic orthoclase (Fig. 11 a).

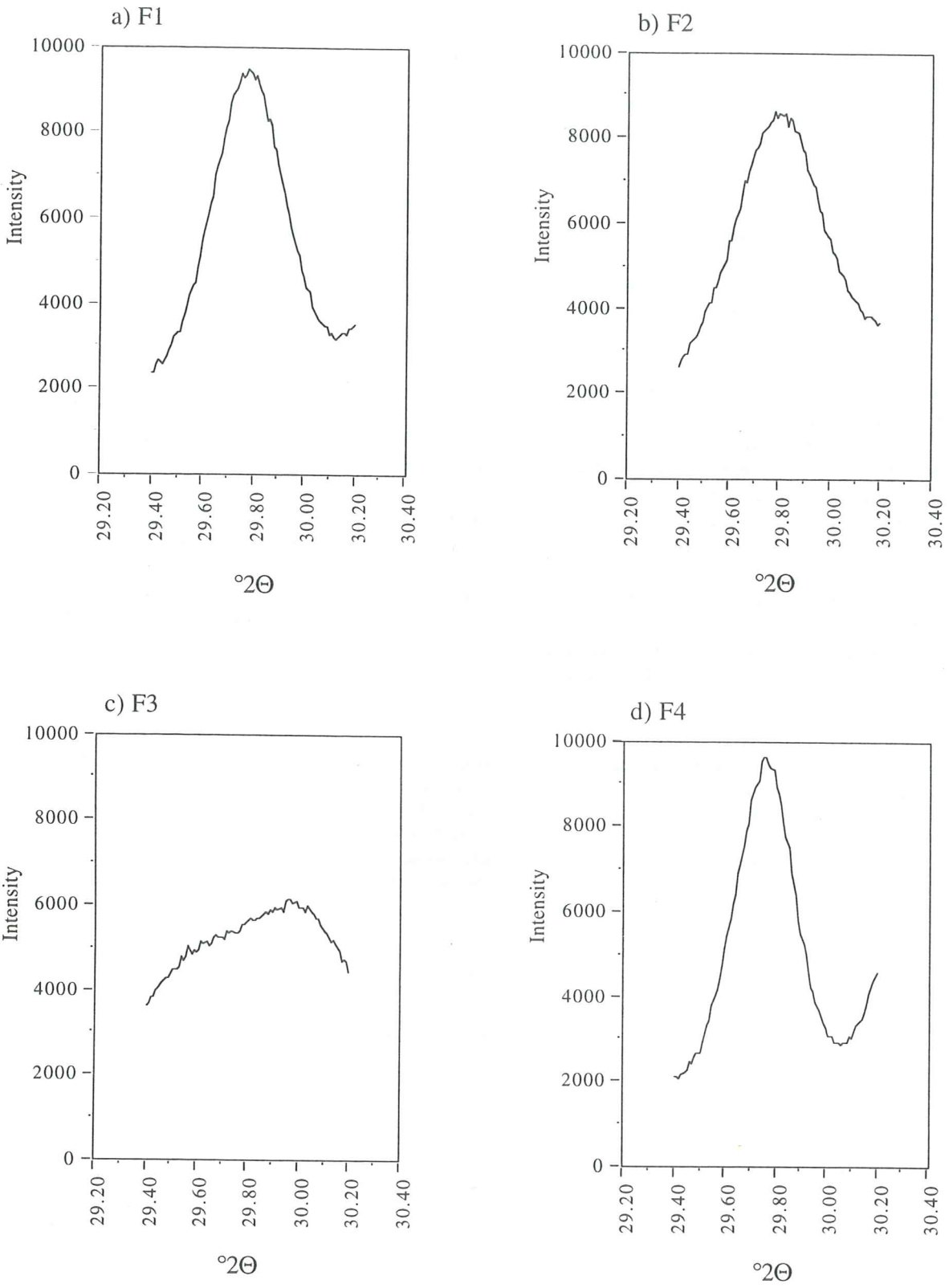

Fig. 12 a-d. X-Ray diffractograms from analyses of K-feldspar megacrysts from the Tjärnesjö granitoids: **(a)** F1 = undeformed granite; **(b)** F2 = slightly deformed granite; **(c)** F3 = intensely deformed granite; **(d)** F4 = moderately deformed charnockitoid.

6. The Mafic granulites at Svartaberg

Two mafic granulitic dykes have been discovered within the Tjärnesjö granite in the northern parts of the investigated area (Fig 3). The dykes are slightly foliated to almost massive and about 5-10 meters wide. The immediate contacts with the surrounding Tjärnesjö granite are covered, but the intrusive nature of the dykes is clear. The western dyke can be traced about 200 meters in an approximately NNE-direction. Further observations of the extension of the dykes are limited by poor exposure in the area.

Pyroxene, garnet, hornblende, biotite and plagioclase are the most common minerals. Garnet is common in all samples. Pyroxene is present at both localities, though variously retrograded. Biotite is reddish to greyish brown, and in places, on the basis of textural evidence, it is formed due to retrogression of granulite facies metamorphic minerals.

The magmatic mineral assemblages are partly to totally replaced by granulite facies assemblages. Primary pyroxene is replaced by metamorphic clinopyroxene, which in turn is partly replaced by hornblende during a later retrogression. Fine-grained aggregates of pyroxene neoblasts are not affected by amphibolitization. The degree of retrogression varies between the samples, and hornblende may sometimes be absent. Remnants of a magmatic texture, such as the remains of plagioclase needles can be found in places.

7. Chemical composition

No chemical data have previously been published from the Tjärnesjö massif. Four samples from the Tjärnesjö intrusive were analysed to chemically classify the granitoids. The samples were chosen in order to analyse rocks of different appearance within the massif. Sample C1 and C4 were the most well defined granite and charnockitoid respectively, while sample C2 and C3 were selected for comparison. The analyses were made on massive rocks with the exception of sample C4 which displayed obvious foliation. For the location of sample-sites, see Fig 3. The data presented here are far too limited to allow any detailed interpretation of the chemical nature or the petrogenesis of the granitoids at Tjärnesjö.

Tab. 3. Chemical data and CIPW-weight norms for the Tjärnesjö granite, charnockitoid, and rocks from the Varberg Granite Charnockite Association (CGA). For calculation of the CIPW-weight norm of rocks from the CGA, total Fe was correlated with the proportions of Fe^{2+} and Fe^{3+} in the Tjärnesjö Granite (C1) for the Torpa Granite, and the Tjärnesjö Charnockitoid (C4) for the charnockites of the CGA. Key: (C1 and C3) Tjärnesjö granite; (C2 and C4) Tjärnesjö charnockitoid; (TG) Torpa granite; (VC) Varberg charnockite; (TC) Trönningenäs charnockite; (AGC(c)) Apelviken-Getterön charnockite (coarser matrix); (AGC(f)) Apelviken-Getterön charnockite (finer matrix). Chemical data for rocks from the CGA is taken from Hubbard (1989).

Major oxide elements :	C1	C2	C3	C4	TG	VC	TC	AGC(f)	AGC(c)
SiO2 (wt %)	70,04	62,87	69,93	60,55	70,6	58,6	64,3	64,4	63,4
TiO2	0,68	0,79	0,66	1,05	0,5	1,4	1,1	1,2	1,2
Al2O3	14,01	17,64	14,08	17,49	14,1	15,3	15,5	13,1	14,3
Fe2O3	1,56	1,42	1,72	2	3,4	9,6	5,8	7,9	7,3
FeO	2,09	2,74	1,88	3,82	–	–	–	–	–
MnO	0,09	0,11	0,09	0,15	0,1	0,2	0,1	0,2	0,2
MgO	0,57	0,65	0,56	0,89	0,9	1,6	1,4	1,2	1,5
CaO	1,7	3,2	1,71	3,84	1,7	4,3	3,2	2,9	3,2
Na2O	3,52	4,52	3,56	4,7	3,3	4,5	3,8	3,6	3,8
K2O	5,3	4,9	5,23	4,22	5,2	4,1	4,8	4,8	4,7
P2O5	0,25	0,28	0,24	0,47	0,1	0,4	0,2	0,6	0,4
LOI	0,19	0,21	0,17	0,04	–	–	–	–	–
S	100,23	99,64	100,04	99,65	99,5	100	100,2	99,9	100
Ba (ppm)	1315	2365	1347	2277	1140	2167	1457	1522	1472
Nb	14	19	13	19	39	37	50	40	42
Rb	119	86	115	76	192	58	124	86	91
Sr	216	413	219	450	229	298	270	189	210
Zr	453	630	459	569	331	281	369	436	466
Y	33	43	34	49	56	32	51	26	30

CIPW-weight norm:	C1	C2	C3	C4	TG	VC	TC	AGC(c)	AGC(f)
Quartz	24,77	9,68	24,88	7,44	26,07	5,12	14,52	14,12	17,27
Orthoclase	31,32	28,96	30,91	24,94	30,73	24,23	28,37	27,78	28,37
Albite	29,79	38,25	30,12	39,77	27,92	38,08	32,15	32,15	30,46
Anorthite	6,78	13,37	6,92	14,16	7,78	9,44	11,06	8,08	5,41
Diopside	0,02	0,57	0,03	1,53	0	7,82	2,91	4,33	4,28
Hyperstene	3	4,09	2,5	5,35	3,85	6,94	5,74	6,7	6,53
Magnetite	2,26	2,06	2,49	2,9	2,17	4,78	2,9	3,62	3,91
Ilmenite	1,29	1,5	1,25	1,99	0,95	2,66	2,09	2,28	2,28
Apatite	0,58	0,65	0,56	1,09	0,23	0,93	0,46	0,93	1,39
Pl is An	19	26	19	26	22	20	26	20	15

Major oxide and trace element compositions are presented in Table 3. The analyses were made at the analytical laboratory at the Geological Institute, University of Lund. Si, Ti, Al, total Fe, Ca, K, Ba, Rb, Sr, Zr, Nb and Y were all analysed by X-ray fluorescence. Fe^{2+} was determined by potentiometric titration; Mn, Mg and Na, by atomic absorption spectroscopy, and P was spectrophotometrically analysed. Loss on ignition, LOI, was determined by gravimetrical methods. All analyses are referred to as U.S.G.S. standards. For a detailed description of the analytical methods see Solyom et al. (1984). Chemical data including mean values of major oxide components from the Varberg Granite Charnockite Association (Hubbard 1989) were used for comparison (Tab. 3).

The granitoids were classified according to Debon & Le Fort (1983), using the coordinates Q=(Si/3-(K+Na+2Ca/3)) and P=(K-(Na+Ca)). Q broadly represents the quartz-content, and P stands for the proportion of K-feldspar versus the total feldspar content. As shown in Fig. 13, the Tjärnesjö and Torpa granites are true granites, while the Apelviken-Getterön Charnockites (AGC), Trönningenäs Charnockite (TC) and the intermediate Tjärnesjö charnockitoid plot in the quartz-monzonitic field. The Tjärnesjö charnockitoid straddles the boundary to the monzonite field, where the Varberg Charnockite (VC) also plot (Fig. 13).

The Debon & Le Fort (1983) AB-diagram, Fig. 14, defines the aluminous character of the granitoids by using the relation between dark minerals and the Al content relative to the (K+Na+2Ca) content. Parameter A=Al-(K+Na+2Ca) and parameter B=(Fe+Mg+Ti). Na, K and Ca in excess of Al will give the rock a metaluminous character, while peraluminous rocks are under saturated in Na, K and Ca in relation to Al. All the Tjärnesjö granitoids, as well as the granitoids from the Varberg area, fall into the domains of metaluminous rocks. Some differentiation may be traced among the true granites where the Torpa granite (TG) passes slightly into the field of peraluminous rocks. The Tjärnesjö granite is metaluminous but plots closer to the TG position than the Tjärnesjö charnockitoids and the charnockites from CGA.

Differentiating trends in granitoid rocks are discussed by El Bouseily & El Sokkary (1975), using plots of the ternary relations of Rb, Ba and Sr. All granitoids from the Tjärnesjö area and the Torpa granite are concentrated in the field of "anomalous granites", while the charnockites of the CGA also fall into the field of normal granites (Fig. 15).

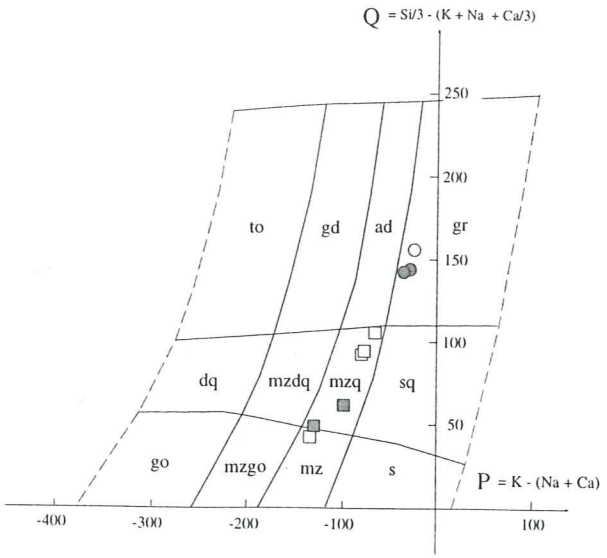

Fig. 13. PQ-diagram according to Debon & Le Fort (1983). Q is proportional to the quartz content. P is proportional to the K-feldspar content relatively the total feldspar ratio. Key: (gr) granite; (ad) adamellite; (gd) granodiorite; (to) tonalite; (dq) quartz-diorite; (mzdq) quartz-monzodiorite; (mzq) quartz-monzonite; (sq) quartz-syenite; (go) gabbro; (mzgo) monzo-gabbro, monzo-diorite; (mz) monzonite; (s) syenite. Filled circles = Tjärnesjö granites. Open circles = Torpa granite. Filled squares = Tjärnesjö charnockitoids. Open squares = charnockites from the Varberg Charnockite Granite Association (CGA).

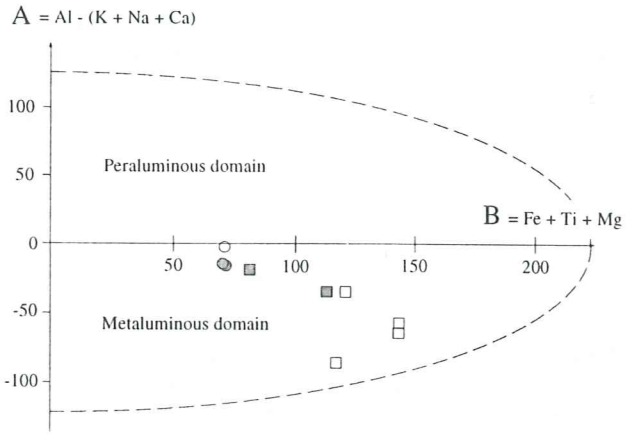

Fig.14. AB-diagram according to Debon & Le Fort (1983). A is a measure of the alumina saturation in the rock and B is roughly proportional to the amount of dark minerals. Symbols as in Fig. 13.

According to El Bouseily & El Sokkary (1975), anomalous granites are referred to as metasomatosed granites. They discuss the possibility of fractionation of Rb due to metamorphic processes, which would cause the variation in Rb content between normal and anomalous granites. However, Lindh & Johansson (1991) argues that primary granitoids of chemical compositions between normal granites and granodiorites would also classify as anomalous granites.

Compositional variation in the granitoids, presented by the log10($CaO/(Na_2O+K_2O)$) vs. wt % SiO_2 plot, proposed by Brown (1981), displays clear alkali-calcic trend, for both the Tjärnesjö granitoids and the granitoids from the CGA (Fig. 16).

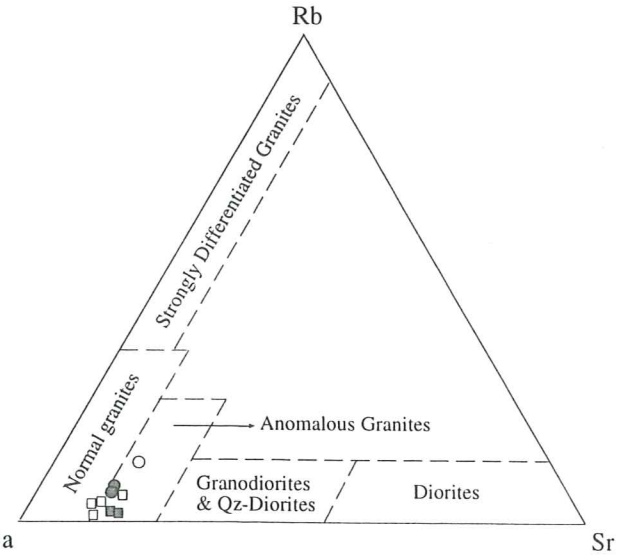

Fig. 15. Rb, Sr and Ba plot according to El Bousley & El Sokkary (1975). Symbols as in Fig. 13.

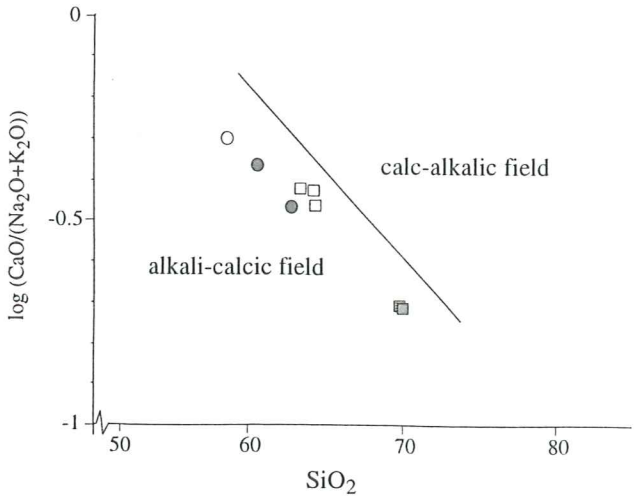

Fig. 16. Log ($CaO/(Na_2O+K_2O)$) vs. SiO_2 (%) plot after Brown (1981). Symbols as in Fig. 13.

8. Age determination.

8.1 Overview

Zircons from the granite, charnockitoid and a pegmatitic dyke were dated by the single zircon evaporation technique (Kober 1986 ,1987). The analyses were carried out at the Laboratory of Isotope Geology at the Museum of Natural History, Stockholm. Isotopic ratios were measured on a Finnigan MAT 261 mass-spectrometer, with a single collector equipped with a Secondary Electron Multiplier (SEM). As the single zircon evaporation technique is still regarded as an unconventional method, it will be described in more detail than the other analytical methods used in this investigation.

8.2 The Pb-Pb single zircon evaporation method.

A zircon is mounted in a canoe-shaped evaporation filament of rhenium. The preferred size is approximately 150 µm. Larger crystals may be used if the zircon is extremely low in U. The filament is then placed in the mass spectrometer and heated stepwise to between 1380-1500° C. This causes release of Pb from different sites in the crystal. Pb together with Si are deposited on the cold ionization filament, which is positioned just opposite the evaporation filament. After collection of Pb for approximately 10-15 minutes, the ionization filament is heated, and Pb is evaporated and transferred into the collector. The Pb isotopes are measured in the mass sequence 206-207-208-206-204, analogous to one scan. Data is then collected in blocks, each comprising ten scans. Generally, two or three data blocks are collected from each Pb-Si deposit. The ionization filament is then cleaned by the raising of the temperature to ca. 1700° C for approximately five minutes, after which a new evaporation-deposit cycle can take place. The evaporation procedure is repeated until the crystal is totally emptied of Pb. For a more detailed description of the Pb-Pb evaporation method, see Kober (1986 and 1987), Chapman & Roddick (1993), Kröner et al. (1994) and Söderlund (in press).

Pb evaporated at low temperatures, i.e. <1500° C, is mainly mobilized from the crystal surface, metamict domains and fractures (Kober 1986). Some of these sites, e.g. metamict domains, may also have been subjected to

radiogenic Pb-loss. This implies that the first evaporation steps of relatively moderate heating often yield disparate $^{207}Pb/^{206}Pb$ ages. At higher temperatures (ca. ≥1500°C), the zircon starts to break down to baddeleyite (ZrO_2) and silica, causing simultaneous release of Pb as the reaction front migrates inwards into the crystal (Chapman & Roddick 1993). Because the retentivity of Pb in intact, crystalline zircon is high, the $^{207}Pb/^{206}Pb$ ages obtained at high-temperature evaporation conditions are often concordant (Kober 1987). From this it follows that an ideal non-complex zircon will retain equal $^{207}Pb/^{206}Pb$ ages from one evaporation step to another, resulting in a so called plateau age with constant $^{207}Pb/^{206}Pb$ ages over several evaporation-deposit cycles.

Complex zircons with more than one age component can sometimes be detected by using the stepwise evaporation technique. This is possible since Pb isotope ratios from different parts of the crystal are analysed separately. The evaporation technique often reveals the nature of complexity, in contrast with the conventional U-Pb dating, by which discordant zircons can be due either to substantial Pb-loss or to mixing of zircons of varying ages.

As the ^{204}Pb is a non-radiogenic isotope, the $^{206}Pb/^{204}Pb$ ratio will reflect the proportion of common lead in the zircon. Originally, a zircon contains nearly negligible amounts of common lead and the Pb present in a zircon will thus mainly be of radiogenic origin. However, during the initial evaporation steps, zircons usually yield relatively low $^{206}Pb/^{204}Pb$ ratios, which increase at higher evaporation temperatures. An originally higher proportion of common lead in the rim than in the core may not always be the explanation, particularly if the $^{207}Pb/^{206}Pb$ ratio is simultaneously increased. Then it is more likely that common Pb has been incorporated in metamict domains and micro fractures which also suffered radiogenic Pb-loss. From this follows that the $^{206}Pb/^{204}Pb$ ratio can be used to detect the occurrence of crystal imperfections such as amorphous, metamict domains or the presence of non-zircon inclusions within the crystal.

The $^{206}Pb/^{208}Pb$ ratio is proportional to the U/Th ratio, which should be similar for zircons of a common origin. Zircons that crystallized from melts associated with anatexis during high-grade metamorphism are usually recognized by a high U/Th content. This is due to a higher mobility of U compared to Th at high grade metamorphic conditions (Constable & Hubbard 1981; Faure 1986; Williams & Claesson 1987). In contrast, magmatic zircons generally have lower U/Th ratios. From this follows that the $^{206}Pb/^{208}Pb$ ratio can be used to distinguish non-complex zircons by comparing the $^{206}Pb/^{208}Pb$ ratios and the $^{207}Pb/^{206}Pb$ ages obtained between the evaporation steps.

8.3 Age calculation and correction of isotopic data

Zircon ages were calculated by repeated testing in Monte Carlo loops of the measured isotopic ratios (computer program designed by M. Hedberg, Stockholm), where the common lead isotope ratios were taken from Stacey and Kramers (1975). Pb-isotope ratios with extreme values were excluded from age calculation, by using a 2σ test (Dixon 1950). Only isotopic data from evaporation steps of uniform $^{207}Pb/^{206}Pb$ ages were used for the age calculation. Mass-scans with low $^{206}Pb/^{204}Pb$ ratios, i.e. below 20.000, were excluded (with the exception of zircons from the charnockitoid sample, see below). Ages are presented at the 2σ confidence level.

8.4 Sampling and zircon preparation

Three different rock units were dated in the Tjärnesjö region: (1) a massive part of the granite; (2) a foliated pyroxene-rich part of the charnockitoid; (3) a pegmatitic dyke which cross-cuts a ductile deformation zone within the granite (Fig. 17). For location of the sample sites, see Fig. 3. Sample weights were ca. 3, 18, and 20 kg., for the granite, the charnockitoid and the pegmatite, respectively. The rock specimens were crushed to a grain-size of less than 300 μm. High density minerals were recovered by using the Wilfley panning table and density fractionation in a heavy liquid (Tetrabrommetan). Magnetic minerals were removed by using the Franz magnetic separator. The almost pure zircon sample was then studied under the microscope and crystals were handpicked.

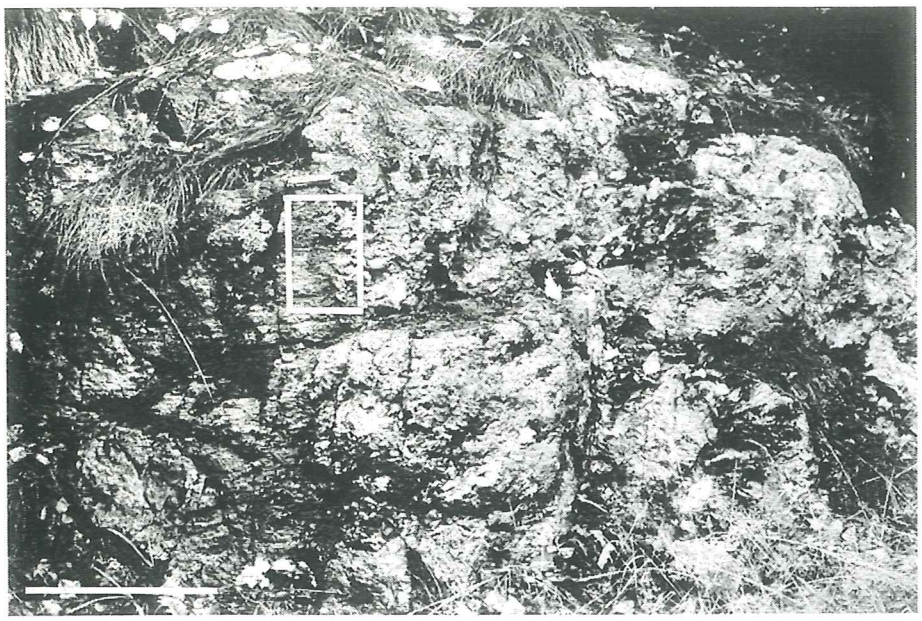

Fig. 17. (a) Pegmatitic dyke crosscutting the gneissosity in an intensely deformed part of the Tjärnesjö granite. The dyke was sampled for age determination (cf. section 8.4 Sampling and zircon preparation). Length of scale is ca. 0.5 m. **(b)** Detailed view showing a magnification of the insert frame in (a).

Fig. 17 a

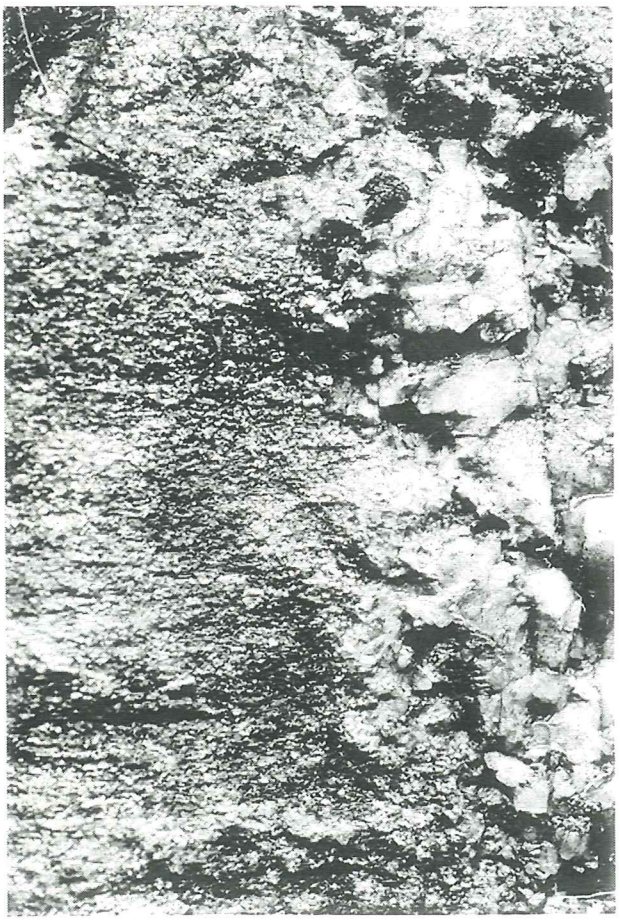

Figure 17 b

8.5 Zircon morphology

8.5.1 Zircons from the granite

Zircons from the granite are mainly prismatic, which is typical for magmatic zircons. Length/width ratios generally vary between 3 and 4. No visible cores are observed under the microscope. Minor, commonly dark inclusions are abundant in the otherwise clear and translucent crystals. Fractures and microscopic cracks are common. Larger grains (≈300 μm) are less elongated and appear somewhat more cloudy compared to the average zircon population. Opaque, cloudy and turbid zircons were avoided, since such features may indicate metamictisation or accommodation of cores. Small grains, around 50 μm are somewhat more rounded, with length/width ratios between 2 and 3. Well rounded, small, poly-facetted grains, typical for metamorphic zircons (Kröner et.al. 1994) have not been observed.

Four zircons, about 100-200 μm in size, were selected for age determination. These grains were transparent and prismatic in shape. Length/width ratios varied between 4 and 5. Zircon G1 was slightly clouded compared to the rest.

8.5.2 Zircons from the charnockitoid

Zircons from the charnockitoid are similar to the zircons in the granite. They are, however, slightly yellowish in colour. Two crystals were selected for age determination, in order to determine the chronological relationship between the charnockitoid and the granite.

8.5.3 Zircons from the pegmatite

The zircons from the pegmatite are prismatic but slightly rounded, especially the smaller grains, and they vary both in size and brightness. Larger grains (≥ 300 μm, with length/width ratios between 1 and 3) display yellowish, turbid inner parts that appear rounded in refractory liquids. These cores are interpreted to represent inherited grains. The outer parts of the zircons are clear, often with pointed colourless tips, indicating a magmatic over-growth on older, partly resorbed grains.

Eight zircons from the pegmatite were dated. Primarily, zircons without visible cores were selected for age determinations. However, totally translucent grains of appropriate size (ca. 150 μm) were more or less absent. Therefore, also grains with an interior minor cloudiness had to be chosen. From one of the zircons, P1, a translucent and euhedral rim was separated from a turbid, almost opaque core (Fig. 18); only the rim was used for age determination.

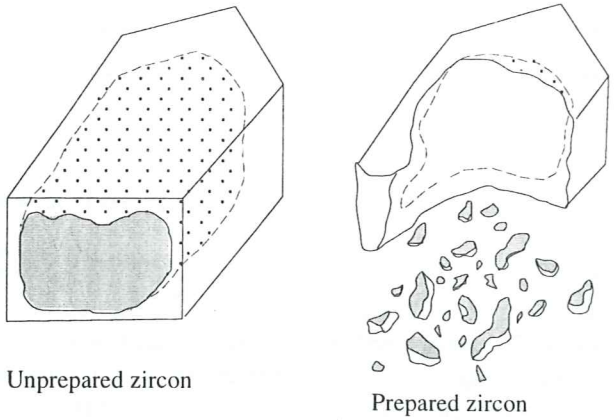

Fig. 18. Sketch visualizing zircon P1 from the Tjärnesjö pegmatite; (**a**) before preparation, (**b**) after preparation, where a translucent euhedral rim was separated from the internal turbid parts. Only the rim was used for age calculation.

8.6 Results and interpretation of isotopic data

8.6.1 The Tjärnesjö granite

Four zircons from the granite sample gave an age of 1361 ± 13 Ma (2σ), which is interpreted to date the granite emplacement (Figs. 19 and 20). All zircons from the granite yielded $^{206}Pb/^{208}Pb$ ratios varying between 6 and 8 (Tab. 4 and Fig. 23).

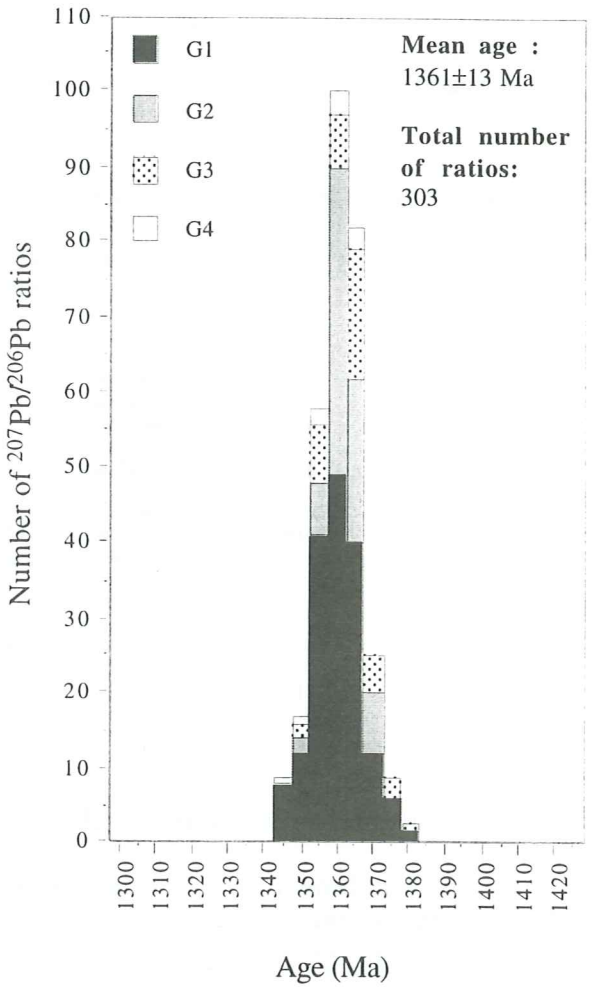

Fig. 19. Histogram showing $^{207}Pb/^{206}Pb$-ages vs. number of scans measured by single-zircon evaporation of four zircons, G1-G4, from the Tjärnesjö granite.

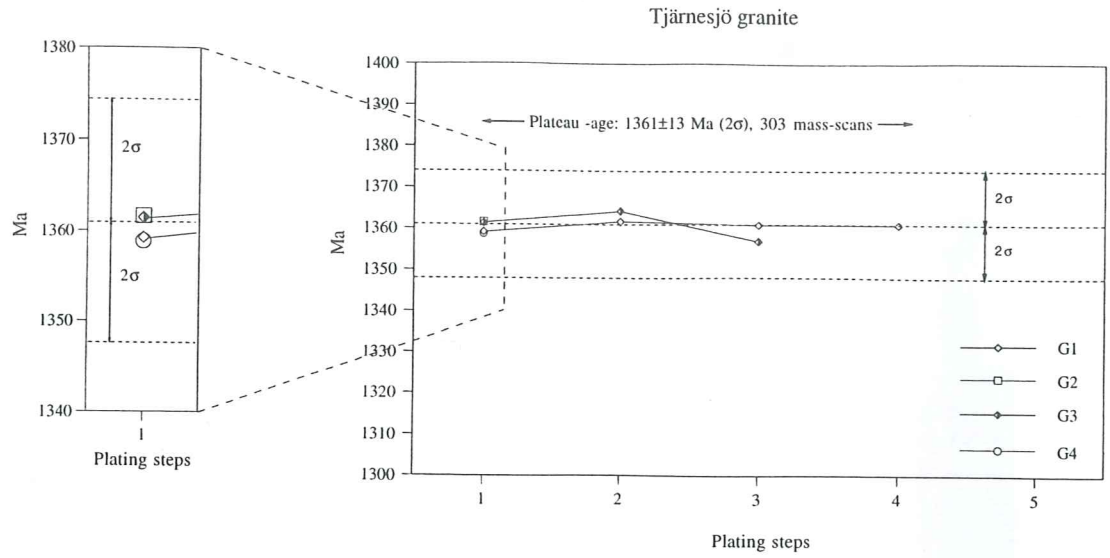

Fig 20. Diagram showing age vs. plating steps from Pb-Pb single-zircon evaporation of four zircons (G1-G4) from the Tjärnesjö granite. Only plating steps used for age calculation are presented in the diagram. Note that all four zircons are present at the first plating step, which is demonstrated separately by the enlargement of the left part of the diagram.

Tab. 4. Single-zircon analytical data for the Tjärnesjö granite and charnockitoid. * = zircons used for age calculation.

Rock :	Grain :	Evaporation temperature : (°C)	Number of mass-scans :	$\frac{^{206}Pb}{^{204}Pb}$	$\frac{^{206}Pb}{^{208}Pb}$	$\frac{^{207}Pb}{^{206}Pb}$	Age : (Ma)
Granite	G1*	1475	52	95000	6.4	.0870815	1358 ± 7
		1485	65	127000	6.7	.0872507	1363 ± 7
		1485	71	130000	6.7	.0871042	1359 ± 6
Granite	G2*	1485	80	37000	7.3	.0874421	1362 ± 4
Granite	G3*	1470	34	36000	7.8	.0875919	1365 ± 7
		1470	9	22000	7.9	.0875901	1358 ±10
		1500	8	125000	8.1	.0869215	1356 ± 6
Granite	G4*	1460	14	24000	8.1	.0875436	1359 ± 8
Charnockitoid	C1	1520	3	22000	8.2	.0877434	1354 ± 6
Charnockitoid	C2	1510	7	26000	7.5	.0872784	1360 ±14
		1520	8	10000	6.3	.0877000	1346 ± 6

8.6.2 The Tjärnesjö Charnockitoid

Two zircons from the charnockitoid gave an average age of 1353 ± 21 Ma (2σ), which within error is similar to the age of the granite. This age is interpreted as being slightly younger than the real age, which could be supported by $^{206}Pb/^{204}Pb$ ratios below 20.000. All zircons from the charnockitoid gave low $^{206}Pb/^{208}Pb$ ratios, similar to those obtained for the granite (Tab. 4 and Fig. 23). The similarity in age and $^{206}Pb/^{208}Pb$ ratio between the charnockite and the granite suggest that these rocks crystallized from a common magma source.

8.6.3 The Tjärnesjö pegmatite

Two zircons, P1 (recovered rim from a core-bearing crystal) and P2, gave an age of 955 ± 21 Ma (2σ) (Figs. 21 and 22). During analyses, these two zircons showed no variation in isotopic composition between the evaporation steps. The obtained $^{206}Pb/^{204}Pb$ ratios are between ca 30.000 and 45.000. The $^{206}Pb/^{208}Pb$ ratios for P1 are between 210 and 250, and between 115 and 125 for P2 (Tab. 5 and Fig. 23). The age of zircon P1 and P2 is interpreted as the intrusion age of the pegmatitic dyke. The recovered rim from zircon P1 is suggested to be a magmatic

overgrowth, which crystallized on an older, partly resorbed zircon crystal. In contrast, P2 is proposed to be a non-complex entirely magmatic zircon, without any inherited components.

Zircons P3, P4 and P7 gave only one evaporation step each, and the interpretation of these ages is therefore more uncertain. Furthermore, $^{207}Pb/^{206}Pb$ ages from these zircons do not overlap, neither individually nor with ages from zircon P1 and P2 (Tab. 5). Consequently, these crystals were excluded from the age calculation.

Zircons P5, P6 and P8 were also excluded, since the evaporation ages of these crystals failed in reaching any plateaus and instead continued to increase throughout the runs (Tab.5). This indicates that the zircons either suffered severe Pb-loss or that they were complex, i.e. contained components of varying ages. The complex nature of these zircons (P5, P6 and P8, probably also zircons P3, P4 and P7) is favoured because of:

(1) The $^{206}Pb/^{208}Pb$-ratios lie between the $^{206}Pb/^{208}Pb$-ratios for the granite-charnockitoid and the zircons from the pegmatite, P1 and P2. (Fig. 23). This could possibly be an indication that the Tjärnesjö intrusion is the source rock for the pegmatite.

(2) The observations of the interior of the crystals from the pegmatite clearly revealed the presence of older cores.

The $^{207}Pb/^{206}Pb$ ages obtained for zircon P3-P8 are therefore interpreted to represent mixed ages without any geological significance.

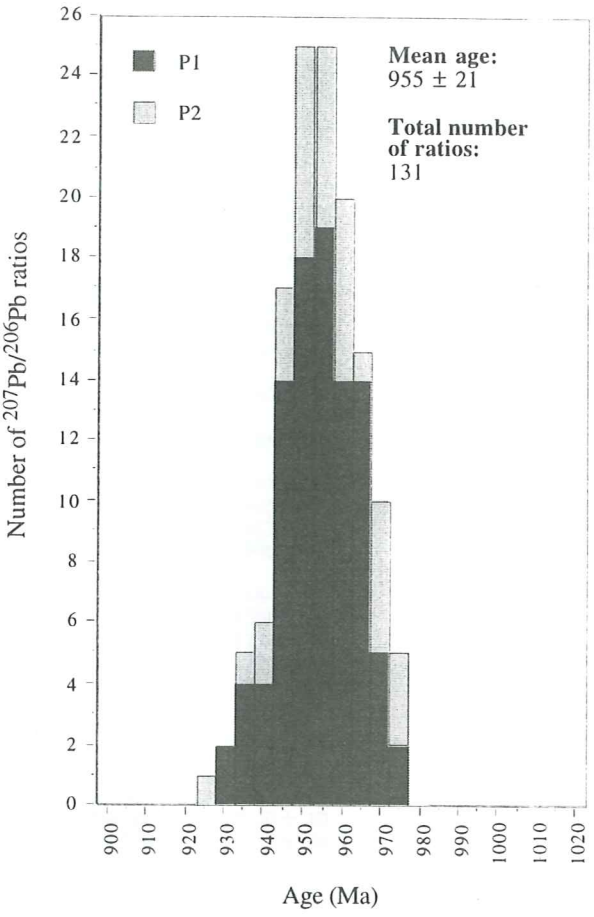

Fig. 21. Histogram showing $^{207}Pb/^{206}Pb$-ages vs. number of scans measured by single zircon evaporation of two zircons, P1 and P2, from the Tjärnesjö pegmatite.

Tjärnesjö Pegmatitic dyke

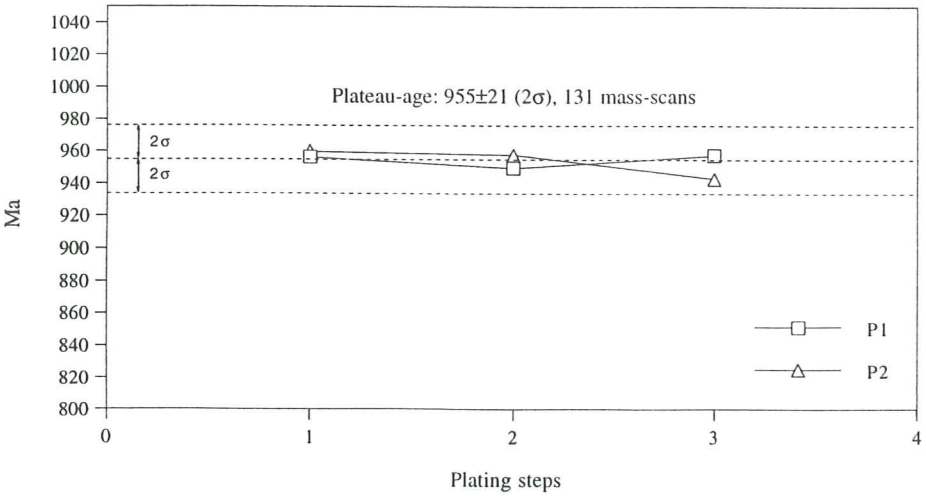

Fig 22. Diagram showing age vs. plating steps from Pb-Pb single-zircon evaporation of two zircons (P1 and P2) from the Tjärnesjö pegmatitic dyke. Only evaporation steps used for age calculation are presented in the diagram.

Tab. 5. Single-zircon analytical data for the Tjärnesjö pegmatitic dyke. * = zircons used for age calculation.

Grain :	Evaporation temperature : (°C)	Number of mass-scans :	$\frac{^{206}Pb}{^{204}Pb}$	$\frac{^{206}Pb}{^{208}Pb}$	$\frac{^{207}Pb}{^{206}Pb}$	Age : (Ma)
P1*	1450	26	33000	209.7	.0714200	956 ± 7
	1450	18	35000	212.3	.0711501	949 ± 7
	>1450	15	29000	247.4	.0712756	950 ± 10
	>1450	37	28000	207.4	.0715243	957 ± 11
P2*	1480	5	43000	115.3	.0714308	960 ± 10
	1480	25	46000	118.5	.0713861	958 ± 11
	>1500	5	37000	122.3	.0709068	943 ± 16
P3	1465	11	11000	89.8	.0727050	967 ± 9
P4	1500	54	9000	46.1	.0736168	986 ± 13
P5	1480	20	35000	171.5	.0712027	947 ± 5
	1510	40	47000	154.0	.0709277	945 ± 9
	1515	30	57000	94.7	.0714642	963 ± 10
	1530	43	47000	46.1	.0723176	986 ± 4
P6	1500	9	3000	11.4	.0841284	1184 ± 15
	>1500	7	13000	9.3	.0840197	1268 ± 13
	>1500	6	24000	8.2	.0838157	1274 ± 3
	>1500	16	24000	8.2	.0846821	1295 ± 18
	>1500	8	30000	8.1	.0848466	1299 ± 12
	>1500	7	114000	7.1	.0856175	1325 ± 8
P7	1450	16	15000	52.7	.0752714	1051 ± 8
P8	1485	19	6000	40.6	.0750947	1000 ± 8
	1510	18	8000	28.9	.0754106	1030 ± 10
	1510	9	10000	26.7	.0752578	1025 ± 56

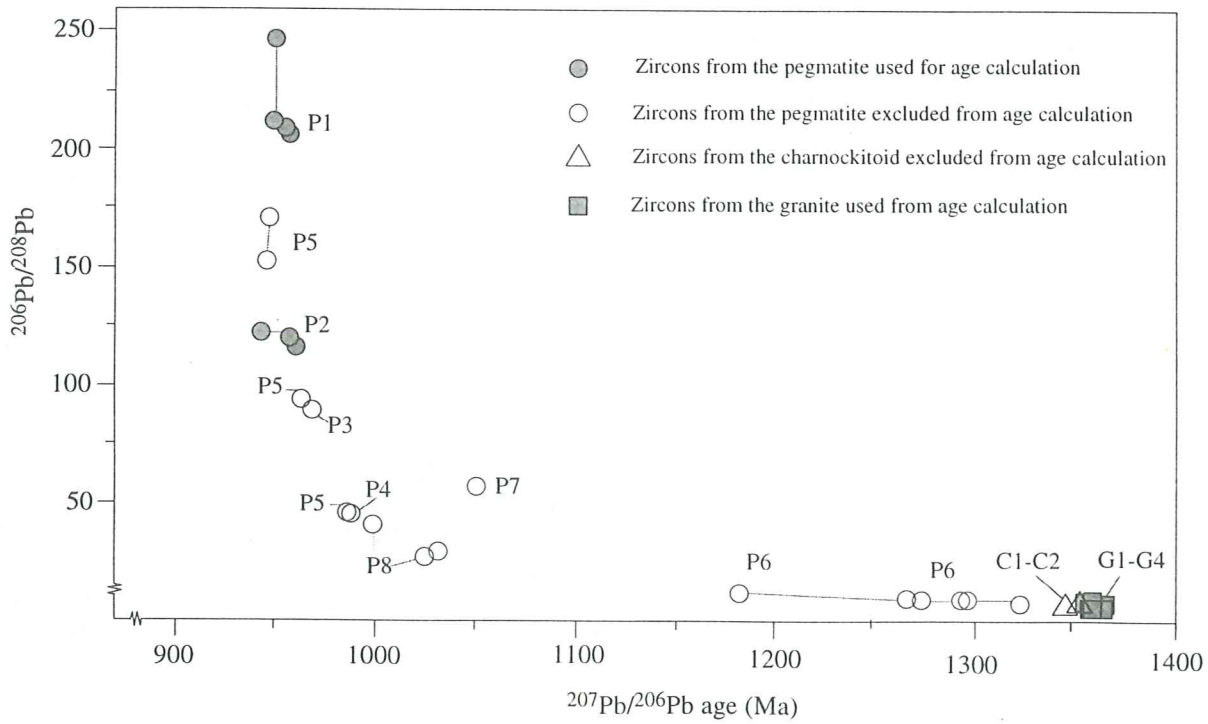

Fig. 23. $^{206}Pb/^{208}Pb$ vs. $^{207}Pb/^{206}Pb$-ages for zircons from the Tjärnesjö granite, charnockitoid and pegmatite. Note that zircons used for age calculation are shown as filled symbols while zircons that were excluded from age calculation are shown as empty symbols.

9. Discussion

9.1. Age of the Tjärnesjö granitoid association and interpretation of the Tjärnesjö charnockitoid

The time interval 1.4-1.2 Ga is characterized by pre-Sveconorwegian "anorogenic" igneous activity in the southwestern parts of the Baltic Shield (Welin & Samuelsson 1987; Åberg 1988). In this period, the ca. 1.36 Ga Tjärnesjö granite and the ca. 1.38 Ga Torpa granite (Åhäll et al. 1992) intruded into the present western parts of the Southwest Swedish Granulite Province (Fig. 2). Subsequently the SGP experienced regional metamorphism at high-grade granulite facies metamorphic conditions in late Sveconorwegian time. Previous researchers have estimated pressures around 9-11 kbar and corresponding temperatures around 700-800° C for this granulite forming event (cf. Johansson et al. 1991 and Wang & Lindh in press).

As for the Tjärnesjö region, the neighbouring gneisses surrounding the granite massif exhibit granulite facies mineral paragenesis and high grade deformation fabrics (Möller & Söderlund submitted). This together with the occurrence of granulite-facies metamorphosed mafic dykes within the Tjärnesjö intrusion (Fig. 3) clearly indicate a strong granulite-facies metamorphic overprint throughout the area.

The P-T conditions described above would be sufficient to form charnockitic rocks provided that the P_{H2O} conditions are reasonably low (Allen et al. 1985; Burton & O'Nions 1990; Yoshida et al. 1991; Perchuk & Gerya 1993, and references cited in these sources). Hubbard (1989, and references therein) suggests both a metamorphic and magmatic origin for the charnockitic rocks of the Varberg region. The metamorphic charnockites of the Varberg area should then be regarded as true granulite facies metamorphic rocks. As for the pyroxene bearing units at Tjärnesjö, an originally magmatic charnockitoid character is uncertain. However, the present metamorphic character of the charnockitoids at Tjärnesjö is clearly indicated by the presence of metamorphic granulite facies minerals such as garnet and clinopyroxene. These rocks are consequently regarded as true granulite facies rocks.

The metamorphic nature of the Tjärnesjö garnets is clearly supported by textural evidence, the chemical composition (Prp_{7-9} Alm_{65-67} Grs_{19-20} Sps_{6-7}) and the rich abundance of garnet in the charnockitoids (cf. section 4.3 Petrology & petrography, The Tjärnesjö charnockitoid). In addition, the Tjärnesjö pyroxenes are also interpreted to be metamorphic, and pyroxene can also be observed in textural equilibrium with garnet (Fig. 9). The pyroxenes vary in size and appear in different stages of retrogradation. Large pyroxenes are generally considerably amphibolitized and display clear exsolution lamellae, while small pyroxene neoblasts occur as clear and bright grains without lamellae. However, no difference in chemical composition was detected among the pyroxenes analysed in the charnockitoids. It is therefore suggested that the large pyroxenes are remnants of early pyroxenes, possibly magmatic, but that their present composition reflects reequilibrium to high-grade metamorphic conditions. The present equilibrium is further supported by the existence of small clear, non-retrograded pyroxene neoblasts. The instability of large pyroxenes is explained by the general retrogression of altered metamorphic pyroxenes rich in lamellae.

Hubbard (1989, and references therein) proposed a close genetic relationship between the Torpa granite and the associated charnockitic members of the Varberg CGA. Similarly, age data and field observations presented in this study indicate that the granitoid members of the Tjärnesjö intrusion evolved from a common origin.

However, to fully characterize the nature of the pyroxene-bearing rocks in the Tjärnesjö area, further investigation of the chemistry, mineral assemblages, the distributions of REE elements and isotopes is necessary. It is also very important to study the role of fluids in order to understand the charnockitoid forming process at Tjärnesjö.

The influence of high grade metamorphism is generally hard to estimate in true granites, due to their chemical and mineral composition. Unless the granite is not extremely dry, the granite mineralogy may be stable within wide P-T intervals, where typical high-grade mineral associations like pyroxene and garnet are still absent. The absence of pyroxene-bearing units in the true granites of Tjärnesjö could therefore be explained by the bulk chemistry of the rock and the presence of volatile components, rather than the absence of a Sveconorwegian metamorphic influence. Analysed pyroxene-bearing rocks within the granitoid formation are pyroxene-normative quartz-monzonites, and the importance of the bulk-chemistry controlling the pyroxene-forming processes is further supported by textural and compositional mineralogical similarities between the different granitoid

components of the massif. Examples of such similarities are the uniform chemical composition of hornblendes and the occurrence of recrystallized fine-grained domains associated with brittle deformed, large orthoclase megacrysts occurring in the granite as well as in the charnockitoid.

9.2 Structures and Sveconorwegian deformation

Previous researchers in the region have claimed that intense reworking of preexisting crust and high-grade metamorphism occurred during the late Sveconorwegian in southwestern Sweden (cf. Johansson et al. 1991; Johansson & Kullerud 1993; Möller & Söderlund submitted; Wang & Lindh in press; Wang et al. in prep.; Page et al. in prep.). The intensity and extension of the deformation is still a controversial subject. The Tjärnesjö massif as well as the Varberg CGA are surrounded by high grade, veined to migmatitic gneisses. The prehistory of the surrounding rocks, the degree of deformation and metamorphism are not known, although the intruding ca. 1.36-1.38 Ga granitoids set the minimum age of the majority of the adjacent gneisses. However, based on work just cited and on recent work by Möller & Söderlund (submitted), it is evident that the country rocks were deformed and metamorphosed during the Sveconorwegian event, at P-T conditions sufficiently high to cause substantial reworking and even partial melting. A minimum age for the regional foliation exposed in Tjärnesjö is set by the occurrence of undeformed, pegmatitic dykes that cross-cut the gneissosity in both the gneisses and the granitoids. The dated pegmatitic dyke at Tjärnesjö gave an age of ca. 955 Ma; similarly, an undeformed granitic dyke at Gällared (Fig. 2), which truncates the gneissosity of a retrograded mafic granulite, has been dated at ca. 956 Ma (Möller & Söderlund submitted). These ages are minimum ages of the regional foliation, while the ca. 1.36 Ga age of the Tjärnesjö intrusive sets the maximum age for the regional foliation that affected the granitoids. Consequently the regional high-grade metamorphism and deformation of the Tjärnesjö massif is interpreted to be late Sveconorwegian.

9.3 Heterogeneous deformation and K-feldspar transformation.

As mentioned above large parts of the investigated area of the Tjärnesjö intrusion are foliated. The deformational pattern is very heterogeneous, varying from gently deformed to intensely deformed sometimes protomylonitic, rocks. The variation in response to deformation shown by the K-feldspar megacrysts is another interesting heterogeneity within the granitoids. X-ray diffraction analysis of K-feldspar reveals the structural conversion of monoclinic orthoclase into a mixed crystalline state with components of triclinic microcline in deformed rocks. The transformation of the orthoclase phase is accentuated as the degree of deformation increases, but "microclinization" may be traced even in rather gently deformed rocks. However, large deformed units within the massif, generally in the more homogeneously foliated central parts show no transformation of the orthoclase. In fact, the most well defined orthoclase phase was discovered in a gneissic part of the charnockitoid. In such deformed rocks where the orthoclase crystals retain their crystallographic nature, they may appear fractured, surrounded by fine grained recrystallized domains of quartz, plagioclase and myrmekite. The preservation of the orthoclase phase in these gneissic units suggests an early stage of deformation at high temperature conditions where orthoclase is stable, followed by deformation at a lower temperature, represented by the heterogeneously foliated, discrete deformation zones associated with microclinization of the K-feldspar.

High-grade garnet-clinopyroxene-bearing mineral assemblages define the foliation in the gneissic charnockitoids and the orthoclase crystals are stable within these rocks. Surrounding deformed granitoids, where the feldspars are progressively transformed into intermediate microcline, may in places contain remnant garnet but lack pyroxene. This confirms an event of a high-grade deformation, followed by a second deformational phase of a retrograde character.

The character of the deformation within the massif is obviously complex. The differences in competence between the granitoid units, e.g. textural differences as variation in grain size and the amount of megacrysts and the influence from fluids e.t.c., are other important factors that control the response to deformation within the intrusive. However, study of these factors is beyond the scope of the present work.

10. Conclusions

1) The Tjärnesjö granite was dated by the Pb-Pb evaporation method. The age of 1361 ± 13 Ma is interpreted as the age of the granite emplacement. Zircons from charnockitoid units gave similar ages, i.e. around 1360 Ma.

2) Alkali-calcic magmatism characterizes the granitoid complex, where the Tjärnesjö granite is a true granite and the associated charnockitoids have a quartz-monzonitic composition. A metaluminous trend is common for all the analysed granitoids. The interpretation of the chemical nature of the granitoids is preliminary since it is based on only a few analyses.

3) The rocks of the Tjärnesjö granite massif are suggested to have undergone two stages of deformation. The first deformation took place at high temperature, and the associated foliation is characterized by stable orthoclase and in charnockitoid units by the presence of metamorphic garnet and clinopyroxene. A second deformational phase which took place at lower temperature conditions caused structural conversion of orthoclase into a mixed state with components of microcline, and possibly also local retrogradation of pyroxene-bearing units.

4) A ca. 955 Ma old undeformed discordant pegmatitic dyke in a gneissic part of the granite sets the minimum age of the deformation that affected the massif. The ca. 1361 Ma intrusion age of the granite gives a maximum age of the deformation that affected the granitoids.

5) Clinopyroxene and garnet occur in the foliation planes of the charnockitoids at Tjärnesjö, and garnet and clinopyroxene also replace the magmatic minerals in mafic dykes, which intruded the massif. This metamorphic and textural evidence clearly demonstrates that the Tjärnesjö intrusion was affected by the Sveconorwegian high-grade metamorphic event, recognized earlier in other parts of the Southwest Swedish Granulite Province.

6) The correlation between the ca. 1.36 Ga Tjärnesjö granite and the ca. 1.38 Ga Torpa granite in the Varberg region further to the west is admitted not only by the intrusive ages, but also by similarities in the bulk chemistry and the general textural appearance of the two massifs.

Acknowledgements

First of all I would like to thank my supervisor Leif Johansson for introducing me to the subject and for enthusiastic guidance. Stefan Claesson and staff at the Laboratory of Isotope Geology at the Museum of Natural History, Stockholm, are gratefully thanked for access to the massspectrometer. Ulf Söderlund for help with age determinations and besides fruitful discussions, encouraging support. Maria Mannestrand for invaluable help with the X-ray diffraction analyses and Mats Eriksson for critical reviews of my work. Anders Lindh, Per-Gunnar Andreasson and Charlotte Möller read and improved the manuscript with valuable comments. Special gratitude is also expressed to Karl-Olov Gustavsson, Varberg, who was the first to notify the special character of the granitoids at Tjärnesjö. Claire E. Gronemeyer improved the English.

References

Åberg, G., 1988: Middle Proterozoic anorogenic magmatism in Sweden and worldwide. *Lithos 21,* 279-289.

Åhäll, K.-I., Samuelsson, L. & Persson, P.-O., 1992: The age of the Torpa granite and its implications for the metamorphism in the Varberg region, SW Sweden. *Geologiska Föreningens i Stockholm Förhandlingar 114,* 449-450.

Allen, P., Condie, K.C. & Narayana, B.L., 1985: The geochemistry of prograde and retrograde charnockite-gneiss reactions in southern India. *Geochimica et Cosmochimica Acta 49,* 323-336.

Andersson, U.B., Larsson, L. & Wikström, A., 1992: Charnockites, pyroxene granulites, and garnet-cordierite gneisses at a boundary between Early Svecofennian rocks and Småland-Värmland granitoids, Karlskoga, southern Sweden. *Geologiska Föreningens i Stockholm Förhandlingar 114,* 1-15

Brown, C.G., 1981: Space and time in granite plutonism. *Philosophical Transactions Royal society London A 301,* 321-336.

Burton, K.W. & O´Nions R.K., 1990: The timescale and mechanism of granulite formation at Kurunegala, Sri Lanka. *Contributions to Mineralogy and Petrology 106,* 66-89.

Chapman, H.J. & Roddick, J.C, 1993: Kinetics of Pb release during the zircon evaporation technique. *Earth and Planetary Science Letters 121,* 601-611.

Constable, J.L. & Hubbard, F.H., 1981: U, Th, and K distribution in a differentiated charnockite-granite intrusion and associated rocks from SW Sweden. *Mineralogical Magazine 44,* 409-415.

Dada, S.S, Briqueu, L., Harms, U., Lancelot, J.R. & Matheis, G., 1995: Charnockitic and monzonitic Pan-African series from north-central Nigeria: Trace-element and Nd, Sr, Pb isotope constraints on their petrogenesis. *Chemical geology 124,* 233-252.

Debon, F. & Le Fort, P., 1983: A chemical-mineralogical classification of common plutonic rocks and associations. *Transactions of the Royal Society of Edinburgh: Earth Science 73,* 135-149.

Deer, W.A., Howie, R.A, & Zussman, J. (eds.) 1978: *Rock-forming minerals. Vol. 2A. single chains silicates.* 1-667 pp. 2nd edition. Longman Group Limited, London.

Dixon, W.J.,1950: Analyses of extreme values. *The Annals of Mathematical Statistics 21,* 488-506.

El Bouseily, A.M. & El Sokkary, A.A., 1975: The relation between Rb, Ba and Sr in granitic rocks. *Chemical geology 16,* 207-219.

Faure, G., 1986: *Principles of Isotope Geology.* 1-589 pp. 2nd edition. John Wiley & Sons, London.

Gaál, G. & Gorbatschev, R., 1987: An outline of the Precambrian evolution of the Baltic Shield. *Precambrian Research 35,* 15-52.

Goldsmith, J.R. & Laves, F., 1954: Potassium feldspars structurally intermediate between microcline and sanidine. *Geochimica et Cosmochimica Acta 6*, 100-118.

Holland, T.H., 1900: The charnockite series, a group of archaean hypersthenic rocks in Peninsular India, *Memoirs of the Geological Survey of India 28*, 119-249.

Hubbard, F.H., 1975: The Precambrian crystalline complex of south-western Sweden. The geology and petrogenetic development of the Varberg region. *Geologiska Föreningens i Stockholm Förhandlingar 97,* 223-236.

Hubbard, F.H., 1978: Geochemistry of the Varberg granite gneisses. *Geologiska Föreningens i Stockholm Förhandlingar 100,* 31-38.

Hubbard, F.H. & Whitley, J.E., 1979: REE in charnockite and associated rocks, southwest Sweden. *Lithos 12,* 1-11.

Hubbard, F.H., 1989: The geochemistry of Proterozoic lower-crustal depletion in southwest Sweden. *Lithos 23,* 101-103.

Janardhan, A.S., Newton, R.C & Smith, J.V., 1979: Ancient crustal metamorphism at low *p*H2O: charnockite formation at Kabbaldurga, south India. *Nature 278,* 511-514.

Johansson, L. & Johansson, Å., 1993: U-Pb age of titanite in the Mylonite Zone, southwestern Sweden. *Geologiska Föreningens i Stockholm Förhandlingar 115,* 1-7.

Johansson, L. & Kullerud, L., 1993: Late Sveconorwegian metamorphism and deformation in southwestern Sweden. *Precambrian Research 64,* 347-360.

Johansson, L., Lindh, A. & Möller, C., 1991: Late Sveconorwegian (Grenville) high-pressure granulite facies metamorphism in southwest Sweden. *Journal of Metamorphic Geology 9,* 283-292.

Kilpatrick, J.A. & Ellis, D.J., 1992: C-type magmas: igneous charnockites and their extrusive equivalents. *Transactions of the Royal Society of Edinburgh: Earth Science 83,* 155-164.

Kober, B., 1986: Whole-grain evaporation for $^{207}Pb/^{206}Pb$-age-investigations on single zircons using a double-filament thermal ion source. *Contributions to Mineralogy and Petrology 93,* 482-490.

Kober, B., 1987: Single zircon evaporation combined with Pb^+ emitter bedding for $^{207}Pb/^{206}Pb$-age investigations using thermal ion mass spectrometry, and implications to zirconology. *Contributions to Mineralogy and Petrology 96,* 63-71.

Kröner, A., Jaeckel, P. & Williams, I.S., 1994: Pb-loss patterns in zircons from a high-grade metamorphic terrain as revealed by different dating methods: U-Pb and Pb-Pb ages for igneous and metamorphic zircons from northern Sri Lanka. *Precambrian Research 66*, 151-181.

Le Maitre, R.W. (ed.), 1989: *A Classification of Igneous Rocks and Glossary of Terms. Recommendations of*

the International union of Geological sciences Subcommision on the Systematics of Igneous Rocks. 1-204 pp. Blackwell Scientific Publications, Oxford.

Leake, B.E., 1978: Nomenclature of amphiboles. *Mineralogical Magazine 42*, 533-563.

Lindh, A. & Johansson, I., 1991: proterozoic granitoids in the Baltic shield- the chemical composition of the Hinneryd granite. *Geologiska Föreningens i Stockholm Förhandlingar 113,* 171-181.

MacKenzie, W.S., 1954: The orthoclase-microcline inversion. *Mineralogical Magazine 30*, 354-366.

[Mannerstrand, M., 1992: *Röntgenkaraktärisering och optisk undersökning av kalifältspater från Varbergs charnockiten och Hinnerydsgraniten, sydvästra Sverige.* Examensarbete i geologi vid Lunds universitet. 46pp.]

Michibayashi, K., 1996: The role of intragranular fracturing on grain size reduction in feldspar during mylonitization. *Journal of Structural Geology 18,* 17-25.

Möller, C. & Söderlund, U. 1996: Age constraints on the regional deformation within the Eastern Segment, SW Sweden, Late Sveconorwegian granite dyke intrusion and metamorphic-deformational relations. Submitted to Geologiska Föreningens i Stockholm Förhandlingar.

Newton, R.C, Smith, J.V. & Windley, B.F. 1980: Carbonic metamorphism, granulites and crustal growth. *Nature 288,* 45-50.

Perchuk, L.L. & Gerya, T.V., 1993: Fluid control of charnockitization. *Chemical geology 108,* 175-186.

Petersen, J.S., 1980: Rare-Earth Element Fractionation and Petrogenetic Modelling in Charnockitic Rocks, Southwest Norway. *Contributions to Mineralogy and Petrology 73,* 161-172.

Quensel, P., 1950: The Charnockite series of the Varberg district on the soth-western coast of Sweden. *Kungliga Svenska Vetenskapsakademien. Arkiv för Mineralogi och Petrologi 1*, 227-332.

Sobolev, N.V., 1964: Classification of rock-forming garnets. *Doklady Akademii Nauk SSSR 157,* 79-84.

Söderlund, U., in press: Conventional U/Pb dating versus single-grain Pb evaporation dating of complex zircons from pegmatite in the high-grade gneisses of south western Sweden. *Lithos .*

Solyom, Z., Andreasson, P. G., Johansson, I. & Hedvall, R., 1984: Petrochemistry of late Proterozoic rift volcanism in Scandinavia: I. the Blekinge-Dalarna Dolerites (BDD)-volcanism in a failed arm of Iapetus? *Lund Publications in Geology 23,* 1-56.

Srivastava, P. & Mitra, G., 1996: Deformation mechanisms and inverted thermal profile in the North Almora Thrust mylonite zone, Kumaon Lesser Himalaya, India. *Journal of structural Geology 18,* 27-39.

Stacey, J.S. & Kramers, J.D., 1975: Approximation of terrestrial lead isotope evolution by a two-stage model. *Earth and Planetary Science Letters 26,* 207-221.

Streckeisen, A., 1974: Classification and Nomenclature of Plutonic Rocks. *Geologische Rundschau 63,* 773-786.

Streckeisen, A., 1976: To each plutonic rock its proper name. *Earth Science Review 12,* 1-33.

Talbot, C.J. & Heeroma, P., 1989: Cover/basement relationships in the SW Swedish gneisses near Varberg. *Geologiska Föreningens i Stockholm Förhandlingar 111*, 105-119.

Wahlgren, C.H., Cruden, A.R. & Stephens, M.B., 1994: Kinematics of a major fan-like structure in the eastern part of the Sveconorwegian orogen, Baltic Shield, south-central Sweden. *Precambrian Research 70,* 67-91.

Wang, X. & Lindh, A., in press: Temperature-pressure Investigation of the Southern Part of the Southwest Swedish Granulite Region. *European Journal of Mineralogy 8.*

[Wedding, B., 1987: *Granatförande pegmatiter i SV Värmland. En mineralogisk och kemisk studie.* Examensarbete i geologi vid Lunds Universitet. 28 pp.]

Welin, E. & Samuelsson, L., 1987: Rb-Sr and U-Pb isotope studies of granitoid plutons in the Göteborg region, sothwestern Sweden. *Geologiska Föreningens i Stockholm Förhandlingar 109*, 39-45.

Williams, I.S. & Claesson, S.; 1987: Isotopic evidence for the Precambrian provenance and Caledonian metamorphism of high grade paragneisses from the Seve Nappes, Scandinavian Caledonides. *Contributions to Mineralogy and Petrology 97,* 205-217.

Yoshida, M., Santosh, M. & Shirata, H., 1991: Geochemistry of Gneiss-Granulite Transformation in the "Incipient Charnockite" Zones of Southern India. *Mineralogy and Petrology 45*, 69-83.

Tidigare skrifter i serien "Examensarbeten i Geologi vid Lunds Universitet":

1. Claeson, Dick & Nilsson, Magnus: Beskrivning av relationer mellan karlshamnsgraniten och leukograniten i Blekinge. 1984.
2. Möller, Charlotte: Eklogitiska bergarter i Roan, Vestranden, Norge. En mineralinventering och texturstudie. 1984.
3. Simeonov, Assen: En jämförelse mellan Jorandomens tennanomala graniters och revsundsgranitens (Västerbotten) mineralogiska och petrografiska karaktär. 1984.
4. Annertz, Kristian: En petrografisk karakteristik av en sent postorogen mafisk intrusion i östra Värmland. 1984.
5. Sandström, Klas: Kartläggning av grundvattenförhållandena i ett delområde av provinsen Nord Kordofan, Sudan. 1984.
6. Gustafsson, Bengt-Olof & Ralfsson, Staffan: Undersökning av högsta kustlinjen på Rydsbjär vid Margareteberg i södra Halland. 1985.
7. Helldén, Johan & Nilsson, Anna-Greta: Undersökning av den baltiska moränleran vid Svalöv, NV-Skåne. 1985.
8. Persson, Karin: Kobolt i pyrit från Kiruna Järnmalmsgruva. 1985.
9. Ekström, Jonas: Stratigrafisk och faunistisk undersökning av Vitabäckslerorna i Skåne. 1985.
10. Säll, Eva: Neobeyrichia from the Silurian of Bjärsjölagård. 1986.
11. Markholm, Carl-Owe: Svagt naturgrus och bergkrossmaterial till bärlager. En laboratoriestudie. 1986.
12. Hellström,Carina: Klassifikation av leptiter i malmstråket mellan Ö. Silvberg och Vallberget, Dalarna. 1986.
13. Öhman, Eva: En petrografisk och mineralogisk studie av en komplex gång bestående av metadiabas och kvartskeratofyr i Kiirunavaaragruvan. 1986.
14. Holmberg, Glenn & Johansson, Lena: Sedimentologisk undersökning av de övre glacifluviala avlagringarna i Vombsänkan, södra Skåne. 1986.
15. Thuning, Bengt & Linderson,Hans: Stratigrafi och överplöjning i Bussjö-området, Ystad. 1986.
16. Bergstedt,Erik & Lööf, Arne I.: Naturvärme- och teknik och geologi med en översiktlig kartläggning av tillgångarna i Kalmar län och Västerviks kommun. 1986.
17. Elg, Anette: Investigation of a wollastonite occurence in central Sweden. 1987.
18. Andrésdóttir, Aaudur: Glacial geomorphology and raised shorelines in the Skardsströnd-Saurbauer Area, west Iceland. 1987.
19. Eken, Karin: Geohydrologisk undersökning vid Filborna avfallsupplag i Helsingborg. 1987.
20. Kockum, Kajsa: Alkalisering vid konstgjord infiltration: En vattenkemisk studie i tre vattentäkter i sydöstra Småland. 1987.
21. Wedding, Bengt: Granatförande pegmatiter i SV Värmland. En mineralogisk och kemisk studie. 1987.
22. Utgår.
23. Hammarlund, Dan: Sedimentstratigrafiska och paleohydrologiska undersökningar av Fönesjön och Kalvs Mosse inom Vombslätten, centrala Skåne. 1988.
24. Jansson, Caroline: Basiska bergarter, gångbergarter, sedimentbergarter och breccior i vaggerydssyenit. En undersökning i protoginzonen vid Vaggeryd. 1988.
25. Jerre,Fredrik: Silurian conulariids from the Lower Visby Beds on Gotland. 1988.
26. Svensson, Erik: Upper Triassic depositional environments at Lunnom, northwest Scania. 1989.
27. Vajda, Vivi: Biostratigrafisk indelning av den Mesozoiska lagerföljden i Köpingsbergsborrningen 3, Skåne. 1988.
28. Persson, Arne: En biostratigrafisk undersökning av conodontfaunan i Limbatakalkstenen på lokalen "Stenbrottet" i Västergötland. 1988.
29. Regnell, Mats: Stenåldersmänniskans vegetationspåverkan på Kullaberg, nordvästra Skåne. En paleoekologisk studie. 1988.
30. Siverson, Mikael: Palaeospinacid selachians from the Late Cretaceous of the Kristianstad Basin, Skåne, Sweden. 1989.
31. Mathiasson, Lena: REE i svekofenniska migmatitneosomer och sensvekofenniska graniter från Nyköpingsområdet. 1989.
32. Månsson, Agneta: Kinematic analysis of the basement-cover contact of the western margin of the Grong-Olden Culmination, Central Norwegian Caledonides. 1990.
33. Lagerås, Per: Kontinuitet i utnyttjandet av Baldringes utmarker. En pollenanalytisk studie i Skogshejdan, Skåne. 1991.
34. Rundgren, Mats: Litostratigrafi och paleomiljöutveckling i Langelandselv-området, Jameson Land, östra Grönland. 1991.
35. Björkman, Leif: Vegetationshistorisk undersökning av en för-historisk jordmånsprofil begravd under en stensträng i Rösered, Västergötland. 1991.
36. Holmström, Patrich, Möller, Per, & Svensson, Mats: Water supply study at Manama, southern Zimbabwe. 1991.
37. Barnekow, Lena: Jämförelse mellan hydrometer-, pipett- och sedigrafmetoderna för kornstorleksanalyser. 1991.

38. Ask,Rikard: Rocks of the anorthosite-mangerite-charnockite-granite suite along the Protogine Zone, southern Sweden. 1992.
39. Leander, Per & Persson, Charlotte: En geologisk och geohydrologisk undersökning av Siesjöområdet norr om Sölvesborg. 1992.
40. Mannerstrand, Maria: Röntgenkaraktärisering och optisk undersökning av kalifältspater från Varbergscharnockiten och Hinnerydsgraniten, sydvästra Sverige. 1992.
41. Johansson, Per: Moränstratigrafisk undersökning i kustklintar, NV Polen. 1992.
42. Hagin, Lena: Övergången mellan koronadiabas och eklogit i Seveskollan på Grapesvare, Norrbotten, svenska Kaledoniderna. 1992.
43. Nilsson, Patrik: Caledonian Geology of the Laddjuvaggi Valley, Kebnekaise-area, northern Swedish Caledonides. 1992.
44. Nilsson, Pia: Lateritisering - en process som kan ha orsakat kontinental Fe-anrikning i Skåne under rät-lias. 1992.
45. Jacobsson, Mikael: Depositional and petrographic response of climatic changes in the Triassic of Höllviken-II, southern Sweden. 1993.
46. Christodoulou, Gina: Agglutinated foraminifera from the Campanian of the Kristianstad basin, southern Sweden. 1993.
47. Söderlund, Ulf: Structural and U-Pb isotopic age constraints on the tectonothermal evolution at Glassvik, Halland. 1993.
48. Remelin, Mika: En revision av Hedströms *Phragmoceras*-arter från Gotlands Silur. 1993.
49. Gedda, Björn: Trace fossils and Palaeoenvironments in the Middle Cambrian at Äleklinta, Öland, Sweden. 1993.
50. Månsson, Kristina: Trilobites and stratigraphy of the Middle Ordovician Killeröd Formation, Scania. 1993
51. Carlsson, Patric: A Petrographic and Geochemical Study of the Early Proterozoic, Bangenhuk Granitoid Rocks of Ny Friesland, Svalbard. 1993.
52. Holmqvist, Björn.H.: Stratigrafiska undersökningar i sjön Vuolep Njakajaure, Abisko. 1993.
53. Zander, Mia: Sedimentologisk undersökning av en kvartär deltaavlagring vid övre Jyllandselv, Jameson Land, Östgrönland. 1993.
54. Albrecht, Joachim: Sedimentological and lithostratigraphical investigations in the gravel pit "Hinterste Mühle" at Neubrandenburg, northeastern Germany. 1993.
55. Magnusson, Martin: Sedimentologisk och morfologisk undersökning av Gyllebo-Baskemöllafältet, östra Skåne. 1994 .
56. Holmqvist, Johan: Vittring i en moränjord vid Farabol, NV Blekinge. 1994.
57. Andersson, Torbjörn: A sedimentological study of glacial deposits in the upper Sjællandselv area, Jameson Land, East Greenland. 1994.
58. Hellman, Fredrik: Basement - cover relationships in the Harkerbreen Group of the northern Ny Friesland Caledonides, Svalbard. 1994.
59. Friberg, Magnus: Structures and PT determination of the Caledonian metamorphism of the lower part of the Planetfjella Group in the area around Mosseldalen, northern Ny Friesland, Svalbard. 1994.
60. Remelin, Mika: Palaeogeographic and sedimentation models for the Whitehill-Irati sea during the Permian of South America and southern Africa. 1994
61. Hagman, Mats: Bevattning med avloppsvatten - en hydrogeologisk studie. 1994.
62. Sandström, Olof: Petrology and depositional history of the Campanian strata at Maltesholm, Scania, southern Sweden. 1994.
63. Pålsson, Christian: Middle-Upper Ordovician trilobites and stratigraphy along the Kyrkbäcken rivulet in the Röstånga area, southern Sweden. 1995.
64. Gustafson, Lars: Senkvartär stratigrafi och utveckling i Örseryd, mellersta Blekinge. 1995.
65. Gichina, Boniface M.: Early Holocene water level changes as recorded on the island of Senoren, eastern Blekinge, southeastern Sweden. 1995.
66. Nilson, Tomas: Process- och miljötolkning av sedimentationen i en subglacial läsideskavitet, Järnavik, S. Blekinge. 1996.